

SOLVING GENERALIZED LYAPUNOV EQUATIONS WITH GUARANTEES: APPLICATION TO THE MODEL REDUCTION OF SWITCHED LINEAR SYSTEMS.

MATTIA MANUCCI* AND BENJAMIN UNGER*

ABSTRACT. We present an efficient strategy to approximate the solutions of large-scale generalized Lyapunov equations (GLEs) with rigorous, computable error guarantees. This work is motivated by applications in model order reduction (MOR) of switched linear systems (SLS) in control form, where GLEs play a central role. We analyze how inaccuracies in the numerical solution of GLEs propagate through the MOR procedure and affect the accuracy and reliability of the reduced order model. Furthermore, the classical balanced-truncation error estimate for SLS is neither theoretically nor practically viable, as they rely on restrictive assumptions requiring several linear matrix inequalities (LMI) to be satisfied exactly by numerically computed solutions of the GLEs. To overcome these limitation, we propose a new MOR framework for SLS, called piecewise balanced reduction (PBR). The method is based on solving multiple GLEs and the construction of projection matrices that are piecewise constant in time to appropriately balance and subsequently reduce the SLS. We extend the standard balanced-truncation error bounds and demonstrate that the PBR formulation allows us to control the error arising from the inexact LMI. In addition, our new error bound accounts for the influence of the piecewise constant time-varying projection matrices. Altogether, this renders the PBR approach for SLS applicable to a broad and flexible class of SLS. Numerical experiments are provided to corroborate our theoretical results.

KEYWORDS: generalized Lyapunov equation, model order reduction, switched systems, balanced truncation, error bound

AMS SUBJECT CLASSIFICATION: 65F45, 65F55, 65P99, 93A30, 93A15, 93B99

1. INTRODUCTION

We study the efficient and certified approximation of the *generalized Lyapunov equation* (GLE)

$$\mathbf{A}\mathbf{X} + \mathbf{X}\mathbf{A}^\top + \sum_{j=1}^M \left(\mathbf{N}_j \mathbf{X} \mathbf{N}_j^\top \right) + \mathbf{B}\mathbf{B}^\top = \mathbf{0}, \quad (1.1)$$

where $\mathbf{A}, \mathbf{N}_j \in \mathbb{R}^{n \times n}$, \mathbf{A} is Hurwitz, i.e., its spectrum is contained in the open left-half complex plane, $\mathbf{N}_j \neq 0$ for $j = 1, \dots, M$, and $\mathbf{B} \in \mathbb{R}^{n \times m}$ with m typically much smaller than n . GLEs with these characteristics naturally arise in the context of *model order reduction* (MOR) of bilinear control systems [5, 18] as well as in the context of stochastic differential equations for stability analysis [11]. For a *switched linear system* (SLS) of the form

$$\Sigma_q \quad \begin{cases} \dot{\mathbf{x}}(t) = \mathbf{A}_{q(t)} \mathbf{x}(t) + \mathbf{B}_{q(t)} \mathbf{u}(t), & \mathbf{x}(t_0) = \mathbf{0}, \\ \mathbf{y}(t) = \mathbf{C}_{q(t)} \mathbf{x}(t), \end{cases} \quad (1.2)$$

Date: January 21, 2026.

the authors of [35] introduced a balancing-based MOR method that requires the solution of certain GLEs. In (1.2), $q: \mathbb{R} \rightarrow \mathcal{J} := \{1, \dots, M\}$ is the external switching signal, which we assume to be an element of the set of allowed switching signals

$$\mathcal{S} := \{q: \mathbb{R} \rightarrow \mathcal{J} \mid q \text{ is right continuous with locally finite number of jumps}\}. \quad (1.3)$$

The symbols $\mathbf{x}(t) \in \mathbb{R}^n$, $\mathbf{u}(t) \in \mathbb{R}^m$, and $\mathbf{y}(t) \in \mathbb{R}^p$ denote the *state*, the controlled *input*, and the measured *output*, respectively. The system matrices $\mathbf{A}_j \in \mathbb{R}^{n \times n}$, $\mathbf{B}_j \in \mathbb{R}^{n \times m}$, and $\mathbf{C}_j \in \mathbb{R}^{p \times n}$ correspond to the *ordinary differential equation* (ODE) active in mode $j \in \mathcal{J}$. For the rest of this manuscript, it is assumed that \mathbf{A}_j is Hurwitz for all $j \in \mathcal{J}$. In the following, we will refer to (1.2) as the *full-order model* (FOM). Sample applications of switched systems include robot manipulators, traffic management, automatic gear shifts, and power systems; see, for example, [8] and the references therein.

If (1.2) has to be repeatedly evaluated, for example, in a simulation context for different inputs or switching signals, or if matrix equalities or inequalities using the system matrices \mathbf{A}_j , \mathbf{B}_j , \mathbf{C}_j in the context of synthesis have to be solved, then a large dimension n of the state makes this a computationally expensive task. In such scenarios, one can rely on MOR and replace (1.2) with the *reduced-order model* (ROM)

$$\tilde{\Sigma}_q \quad \begin{cases} \dot{\tilde{\mathbf{x}}}(t) = \tilde{\mathbf{A}}_{q(t)} \tilde{\mathbf{x}}(t) + \tilde{\mathbf{B}}_{q(t)} \mathbf{u}(t), & \tilde{\mathbf{x}}(t_0) = \mathbf{0}, \\ \tilde{\mathbf{y}}(t) = \tilde{\mathbf{C}}_{q(t)} \tilde{\mathbf{x}}(t), \end{cases} \quad (1.4)$$

with $\tilde{\mathbf{A}}_j \in \mathbb{R}^{r \times r}$, $\tilde{\mathbf{B}}_j \in \mathbb{R}^{r \times m}$, $\tilde{\mathbf{C}}_j \in \mathbb{R}^{p \times r}$, and $r \ll n$. In many cases, see for instance [1], the reduced system matrices are obtained via the Petrov–Galerkin projection, i.e., one constructs matrices $\mathbf{V}, \mathbf{W} \in \mathbb{R}^{n \times r}$, satisfying $\mathbf{W}^\top \mathbf{V} = \mathbf{I}_r$, and then defines

$$\tilde{\mathbf{A}}_j := \mathbf{W}^\top \mathbf{A}_j \mathbf{V}, \quad \tilde{\mathbf{B}}_j := \mathbf{W}^\top \mathbf{B}_j, \quad \tilde{\mathbf{C}}_j := \mathbf{C}_j \mathbf{V}. \quad (1.5)$$

The goal of MOR is thus to derive the matrices \mathbf{V}, \mathbf{W} in a computationally efficient and robust way such that the error $\mathbf{y} - \tilde{\mathbf{y}}$ is small in a given norm. One such way, presented in [35], is to solve GLEs to obtain the projection matrices \mathbf{V}, \mathbf{W} and thus the reduced system (1.5). For this reason, efficiently solving the large-scale generalized Lyapunov equation becomes crucial for MOR.

Remark 1.1. Note that one can generalize the switched system (1.2) by introducing a non-singular symmetric positive-definite matrix $\mathbf{E}_j \in \mathbb{R}^{n \times n}$ that multiplies $\dot{\mathbf{x}}(t)$. In fact, our methodology naturally extends to the case $\mathbf{E}_j \neq \mathbf{I}_n$ considering its inversion and treating $\mathbf{E}_j^{-1} \mathbf{A}_j$ and $\mathbf{E}_j^{-1} \mathbf{B}_j$ in an implicit way.

1.1. Main contributions. To deal with the large-scale setting, we apply the stationary algorithm from [43] in combination with a subspace projection framework [45] to solve GLEs; this approach is widely exploited in the literature of GLEs solution approximation. Our first contribution is the derivation of efficient computable error estimates such that, for any prescribed user tolerance tol , the computed approximation $\tilde{\mathbf{X}}$ of \mathbf{X} , where \mathbf{X} is the exact solution of (1.1), satisfies $\|\mathbf{X} - \tilde{\mathbf{X}}\|_2 \leq \text{tol}$; see [Theorem 3.6](#).

Second, we analyze how numerical errors in the approximation of (1.1) can degrade both the quality and stability of the reduced-order model (ROM) in (1.4). For a specific class of switched systems, we demonstrate how to appropriately perturb the approximated solution $\tilde{\mathbf{X}}$, leveraging the error certification provided by our algorithm to ensure that the resulting ROM remains stable while achieving arbitrarily high accuracy; see [Theorem 3.7](#).

The error bound for the balancing approach [35] applied to SLS relies on the assumption that the solution \mathbf{X} of GLEs satisfies certain *linear matrix inequalities* (LMI). This assumption considerably restricts the number of problems in which the MOR strategy of [35] provides error guarantees. Moreover, even if the LMI are satisfied by \mathbf{X} , they may not be satisfied by its numerical approximation $\hat{\mathbf{X}}$. To overcome this limitation, we introduce a novel *piecewise balancing reduction* (PBR) approach for SLS. After discussing the stability conditions of the associated ROM, we derive a novel error bound that accounts for a potentially violated LMI and piecewise constant in time projection basis; see [Section 4](#) and [Theorem 4.3](#).

The effectiveness of our approach is verified in [Section 5](#) through a synthetic example ([Section 5.1](#)) and a switched system arising from the semi-discretization of a parametric *partial differential equation* (PDE) ([Section 5.2](#)).

1.2. Literature review and state-of-the-art. Several works have addressed the approximation of the GLE solution. The existence and uniqueness of the solutions of GLEs are established, for instance, in [12, Thm. 3.6.1], which is essentially based on the operator splitting ideas developed already in [39]. We also mention [46, Lem. 4.2], and for the more general case of generalized Sylvester equations, a similar characterization of solvability in [23, Thm. 2.1]. The interpretation of the solution as Gramians of bilinear and stochastic linear control systems and their relation to energy functionals is discussed in [5]. Conditions for a fast singular value decay of the solution matrix, essential for a low-rank approximation of the solution, have been developed in [4, 23]. In terms of numerical schemes for the solution of GLEs, we mention the ADI-preconditioned Krylov subspace method [10], the bilinear ADI method [4], the alternative linear scheme [25], which can be interpreted as finding \mathcal{H}_2 optimal search directions [3, 7], and the stationary iteration of [43], which we also employ here, where the inner iteration is solved with a suitable increasing accuracy to minimize computational effort.

As one of our main contributions relates to the use of GLE for MOR of continuous-time SLS, we also provide an overview of the literature on MOR for switched ODEs. The authors of [30, 31] propose to construct ROMs for each mode, independent of the other modes, completely ignoring the transition from one mode to another. Moreover, if a state-dependent switching signal is allowed, any approximation of the ODE may be arbitrarily poor. Both phenomena are detailed with examples in [40]. In [47], an approach is proposed based on a set of coupled linear matrix inequalities, which becomes infeasible in a large-scale context. However, matrix inequalities can be used to guaranty the quadratic stability of the ROM and to derive an error bound [34]. Instead of matrix inequalities, [16, 42] propose solving a set of coupled Lyapunov equations to compute Gramians, which can then be used for a balancing-based model reduction. There is no guaranty that this approach has a solution [28], and in a large-scale setting, the computational complexity may be very demanding. If the Gramians for each mode can be diagonalized simultaneously, then classical balanced truncation methods can be adapted, as discussed in [29]. In contrast, the methods reported in [35, 40] rely on reformulating the switched system as a non-switched system by suitably interpreting the switching signal as a control input. In [40], the switched system is recast as a linear system such that standard methods can be applied, while in [35], the system is recast as a bilinear system, and a balanced truncation approach for such systems is employed. In this paper, we closely follow the second strategy. Both the approach yields a priori error guarantees, provided that certain often non-general

assumptions are satisfied. If prior information on the switching sequence is available, then the method in [35] can be further specialized, as reported in [17]. Although we do not pursue this approach, our method can be adapted in a similar way. Interpolation-based techniques are discussed in [38] for hybrid systems and in [2] for switched systems. For a data-driven approach to obtaining reduced models, we refer to [15]. We emphasize that model reduction is closely related to realization theory. For switched systems, the associated connections are illustrated in [33] and the references therein. In [32], the authors discretize the control variable to obtain a switched system of autonomous PDEs that they approximate with ROMs in a model predictive control framework. Finally, we mention the recent work [24] where the authors deal with a certain class of optimal control problems constrained to SLS dynamic. They employ a model predictive control strategy to deal with this problem, and the use of ROM for SLS is crucial for the efficiency of the strategy and thus its applicability in real-time scenarios.

1.3. Organization of the manuscript. After this introduction, we detail the MOR method from [35] in Section 2. In Section 3.2, we show how to enforce error guarantees suitable for the large-scale setting for the stationary iteration algorithm that approximates the solutions in GLEs. Then, in Section 3.3, for a certain class of SLS, we show how to avoid the numerical error in the approximation of (1.1) from deteriorating the accuracy and stability of the reduced switched system (1.4). In Section 4 we propose a novel MOR algorithm for SLS and discuss its advantages with respect to the method of [35]. Finally, we present numerical examples in Section 5.

1.4. Notation. The symbols \mathbf{I}_n and \mathbf{GL}_n denote the identity matrix of size n and the set of $n \times n$ real non-singular matrices, respectively. For $\mathbf{A} \in \mathbb{R}^{n \times n}$, we write $\mathbf{A} \succeq \mathbf{0}$ or $\mathbf{A} \preceq \mathbf{0}$ if \mathbf{A} is positive or negative semidefinite, respectively. If \mathbf{A} has only real eigenvalues, then we denote the i -th largest eigenvalue (singular value) of \mathbf{A} by $\lambda_i(\mathbf{A})$ ($\sigma_i(\mathbf{A})$) and use $\kappa(\mathbf{A}) = \frac{\sigma_1(\mathbf{A})}{\sigma_n(\mathbf{A})}$ to denote the spectral condition number of \mathbf{A} . Finally, $\Lambda(\mathbf{A})$ indicates the spectrum of \mathbf{A} .

2. PRELIMINARIES

In this section, we recall the balancing-based MOR algorithm for SLS proposed in [35]. This method requires the solution of two GLEs.

2.1. Reachability and Observability. We start by introducing the concepts of reachable and observable sets for a continuous time-switching linear system. Let $\phi(t, t_0, \mathbf{x}_0, \mathbf{u}, q)$ denote the state trajectory at time t of the switched system (1.2) starting from $\mathbf{x}(t_0) = \mathbf{x}_0$ with input \mathbf{u} and switching path $q \in \mathcal{S}$ with \mathcal{S} given in (1.3).

Definition 2.1. Let $q \in \mathcal{S}$ be a given switching path. A state $\mathbf{x} \in \mathbb{R}^n$ is called

- (i) reachable via q if there exists a time instant $t_f > t_0$, and an input $\mathbf{u}: [t_0, t_f] \rightarrow \mathbb{R}^m$, such that $\phi(t_f, t_0, 0, \mathbf{u}, q) = \mathbf{x}$;
- (ii) unobservable via q , if there exists an input \mathbf{u} , such

$$\mathbf{C}_q \phi(t, t_0, \mathbf{x}, \mathbf{u}, q) = \mathbf{C}_q \phi(t, t_0, \mathbf{0}, \mathbf{u}, q) \quad \text{for all } t \geq t_0.$$

The reachable and unobservable sets via q , denoted by \mathcal{R}_q and \mathcal{UO}_q , respectively, are the sets of states that are reachable and unobservable via q , respectively. We define the observable set via q of (1.2), denoted by \mathcal{O}_q , as $\mathcal{O}_q := (\mathcal{UO}_q)^\perp$ (note that this definition is

not unique since any complement set, not just the orthogonal one, would be suitable). The set of reachable states \mathcal{R} and the set of observable states \mathcal{O} of (1.2) can be defined as

$$\mathcal{R} := \bigcup_{q \in \mathcal{S}} \mathcal{R}_q \quad \text{and} \quad \mathcal{O} := \bigcup_{q \in \mathcal{S}} \mathcal{O}_q. \quad (2.1)$$

Reachability and observability are crucial in balancing-based MOR. Indeed, the fundamental idea of this type of projection-based MOR is to remove from the systems the states that are difficult to reach and/or difficult to observe; see [1, Cha. 7] for further details.

2.2. Model reduction algorithm: stability and accuracy conditions. The MOR algorithm of [35] proceeds in two steps to compute the projection matrices \mathbf{V} and \mathbf{W} to obtain a ROM for (1.2). First, we have to define the matrices $\mathbf{A} := \mathbf{A}_1$ and $\mathbf{N}_j := \mathbf{A}_j - \mathbf{A}_1$ for $j = 1, \dots, M$ and solve the GLEs

$$\mathbf{A}\mathcal{P} + \mathcal{P}\mathbf{A}^\top + \sum_{j=1}^M \left(\mathbf{N}_j \mathcal{P} \mathbf{N}_j^\top + \mathbf{B}_j \mathbf{B}_j^\top \right) = \mathbf{0}, \quad (2.2a)$$

$$\mathbf{A}^\top \mathcal{Q} + \mathcal{Q}\mathbf{A} + \sum_{j=1}^M \left(\mathbf{N}_j^\top \mathcal{Q} \mathbf{N}_j + \mathbf{C}_j^\top \mathbf{C}_j \right) = \mathbf{0}. \quad (2.2b)$$

Note that the matrix equations in (2.2) are of the form (1.1) by defining $\mathbf{B} := [\mathbf{B}_1, \dots, \mathbf{B}_M]$ for (2.2a) and $\mathbf{B} := [\mathbf{C}_1^\top, \dots, \mathbf{C}_M^\top]$ for (2.2b). The symmetric positive semidefinite solutions $\mathcal{P}, \mathcal{Q} \in \mathbb{R}^{n \times n}$ are known as the Gramians for (1.2) and they satisfy the relation

$$\mathcal{R} = \text{range}(\mathcal{P}) \quad \text{and} \quad \mathcal{O} = \text{range}(\mathcal{Q}), \quad (2.3)$$

with \mathcal{R} and \mathcal{O} as defined in (2.1); see [35, Thm. 3]. Let us emphasize that, at this stage, the ordering of the system modes is somewhat arbitrary, and any reordering is possible.

Second, let $\mathcal{P} = \mathbf{S}\mathbf{S}^\top$ and $\mathcal{Q} = \mathbf{R}\mathbf{R}^\top$ denote the Cholesky decomposition of the Gramians; compute the *singular value decomposition* (SVD) of the product of the Cholesky factors

$$\mathbf{S}^\top \mathbf{R} = [\mathbf{U}_1, \mathbf{U}_2] \begin{bmatrix} \Sigma_1 & \mathbf{0} \\ \mathbf{0} & \Sigma_2 \end{bmatrix} [\mathbf{V}_1, \mathbf{V}_2]^\top, \quad (2.4)$$

and compute the projection matrices \mathbf{V} and \mathbf{W} via

$$\mathbf{V} = \mathbf{S}\mathbf{U}_1 \Sigma_1^{-1/2} \quad \text{and} \quad \mathbf{W} = \mathbf{R}\mathbf{V}_1 \Sigma_1^{-1/2}. \quad (2.5)$$

This procedure is called square-root balanced truncation (see [1, Sec. 7.3]).

To comment on the stability of the ROM derived through the procedure just detailed, we first need to briefly discuss the stability of the SLS in (1.2); for a comprehensive overview on the topic, see [28, Part II]. The first observation is that assuming that each subsystem is asymptotically stable, i.e., that the matrices \mathbf{A}_j are Hurwitz, is no guarantee for the SLS (1.2) to be stable for any $q \in \mathcal{S}$.

Definition 2.2. *The switched linear system (1.2) is called quadratically stable if there exists a positive definite matrix \mathbf{P} such that $\mathbf{A}_j^\top \mathbf{P} + \mathbf{P} \mathbf{A}_j \prec \mathbf{0}$, for all $j \in \mathcal{J}$.*

Quadratic stability plays a crucial role, as it offers a sufficient condition for ensuring the exponential stability of any SLS characterized by stable modes, regardless of the chosen switching signals $q \in \mathcal{S}$, where \mathcal{S} is specified in (1.3). It is important to note that quadratic stability is merely a sufficient condition; a SLS can remain stable for every $q \in \mathcal{S}$ without

necessarily being quadratically stable; see the discussion in [28, Sec. 2.1.4]. The following lemma provides a crucial result for MOR using the projection matrices in (2.5).

Lemma 2.3 ([34, Lem. 12]). *If the matrices \mathcal{P}, \mathcal{Q} used for the construction of the projection matrices \mathbf{V}, \mathbf{W} in (2.5) satisfy either*

$$\mathbf{A}_j \mathcal{P} + \mathcal{P} \mathbf{A}_j^\top + \mathbf{B}_j \mathbf{B}_j^\top \prec \mathbf{0} \quad \text{for all } j \in \mathcal{J}, \quad (2.6a)$$

or

$$\mathbf{A}_j^\top \mathcal{Q} + \mathcal{Q} \mathbf{A}_j + \mathbf{C}_j^\top \mathbf{C}_j \prec \mathbf{0} \quad \text{for all } j \in \mathcal{J}, \quad (2.6b)$$

then the reduced system (1.4) obtained via \mathbf{V} and \mathbf{W} is quadratically stable.

Finally, we recall a key result that offers an error estimate suitable for constructing a ROM using balancing-based MOR, ensuring that the ROM output meets any prescribed accuracy requirements.

Theorem 2.4 ([34, Thm. 6]). *Let Σ_1 in (2.4) be of size $r \times r$, $\Lambda(\Sigma_1) \cap \Lambda(\Sigma_2) = \emptyset$, and let the distinct singular values of Σ_2 be σ_k , with multiplicities m_k , for $k = r+1, \dots, \tilde{n}$. It follows $\tilde{n} \leq n$ and $n = r + \sum_{k=r+1}^{\tilde{n}} m_i$. Suppose \mathcal{P} and \mathcal{Q} satisfy the LMIs*

$$\mathbf{A}_j \mathcal{P} + \mathcal{P} \mathbf{A}_j^\top + \mathbf{B}_j \mathbf{B}_j^\top \preceq \mathbf{0} \quad \text{and} \quad \mathbf{A}_j^\top \mathcal{Q} + \mathcal{Q} \mathbf{A}_j + \mathbf{C}_j^\top \mathbf{C}_j \preceq \mathbf{0} \quad \text{for all } j \in \mathcal{J}. \quad (2.7)$$

Then, for every switching signal $q \in \mathcal{S}$, the output error between the FOM (1.2) and the ROM (1.4), obtained through the projection matrices (2.5), is bounded by twice the sum of the neglected singular values, multiplicities not counted, times the L_2 norm of the input function, i.e.,

$$\|\mathbf{y} - \hat{\mathbf{y}}\|_{L_2} \leq 2 \left(\sum_{k=r+1}^{\tilde{n}} \sigma_k \right) \|\mathbf{u}\|_{L_2}. \quad (2.8)$$

Proof. The proof is derived from [34, Thm. 6]. The unique aspect here is that the original authors did not specifically differentiate between simple and non-simple neglected singular values. Nevertheless, tailoring their proof to encompass this distinction is achieved by reiterating their steps while addressing non-simple singular values. This approach is further elucidated in the subsequent proof of Lemma 4.2, so those steps will not be reiterated here. \square

We conclude that for the quadratic stability of the reduced SLS, compliance with just one set of LMIs is necessary, specifically either (2.6a) or (2.6b). To ensure error guarantees in the reduced approximation, the sets of LMIs presented in condition (2.7) must also be fulfilled. These LMIs are generally less stringent than those for quadratic stability. Consequently, quadratic stability does not inherently ensure that (2.8) is satisfied; conversely, satisfying (2.8) does not inherently ensure the quadratic stability of (1.4).

3. EFFICIENT AND CERTIFIED NUMERICS FOR LARGE-SCALE GLEs

For the large-scale setting, it is crucial to exploit sparsity when available and to use state-of-the-art methods in every step of the MOR algorithm presented in Section 2.2. Besides computational efficiency, we further aim for error certification and thus have to balance the errors of the different approximations. In more detail, we discuss the algorithm used to approximate the solutions of (2.2) and derive efficiently computable error estimates to certify the quality of the approximation in Section 3.2. Then, in Section 3.3, we show

how the provided error estimate can be used to prevent instabilities and deterioration of accuracy in the ROM.

3.1. Solvability and stationary algorithm. The existence and uniqueness of a solution of (1.1) can be studied via Kronecker algebra, i.e., by introducing the matrices

$$\mathcal{L} := \mathbf{I}_n \otimes \mathbf{A} + \mathbf{A} \otimes \mathbf{I}_n \in \mathbb{R}^{n^2 \times n^2} \quad \text{and} \quad \Pi := \sum_{j=1}^M \mathbf{N}_j \otimes \mathbf{N}_j \in \mathbb{R}^{n^2 \times n^2}, \quad (3.1)$$

such that the vectorized form of (1.1) is given by $(\mathcal{L} + \Pi) \text{vec}(\mathbf{X}) = -\text{vec}(\mathbf{B}\mathbf{B}^\top)$. Hence, the GLE (1.1) is uniquely solvable if and only if $\mathcal{L} + \Pi$ is nonsingular.

Instead of solving the linear system directly, we employ the stationary iteration algorithm from [43, Alg. 2.1] to solve the GLE (1.1) numerically; see [Algorithm 1](#). It consists of

Algorithm 1 Stationary iterations for the GLEs (1.1)

Input: Matrices $\mathbf{A}, \mathbf{B}, \mathbf{N}_j$ for $j = 1, \dots, M$

Output: $\tilde{\mathbf{Z}}$ such that $\mathbf{X} \approx \tilde{\mathbf{Z}}\tilde{\mathbf{Z}}^\top$ is an approximation to the solution of (1.1)

- 1: Set $\mathbf{B}_1 := \mathbf{B}$
- 2: Approximately solve $\mathbf{AX} + \mathbf{XA}^\top + \mathbf{B}_1\mathbf{B}_1^\top = \mathbf{0}$ for $\mathbf{X}_1 = \mathbf{Z}_1\mathbf{Z}_1^\top$
- 3: **for** $k = 2, 3, \dots$ **do**
- 4: Set $\mathbf{B}_k := [\mathbf{N}_1\mathbf{Z}_{k-1}, \dots, \mathbf{N}_M\mathbf{Z}_{k-1}, \mathbf{B}_1]$
- 5: Approximately solve

$$\mathbf{AX} + \mathbf{XA}^\top + \mathbf{B}_k\mathbf{B}_k^\top = \mathbf{0} \quad (3.2)$$

for $\mathbf{X}_k = \mathbf{Z}_k\mathbf{Z}_k^\top$

- 6: **if** sufficiently accurate **then** stop
- 7: **end for**

a fixed-point iteration in which we need to solve a classical Lyapunov equation in each iteration. To ensure that [Algorithm 1](#) is feasible and convergent, we make the following assumption; see, for instance, [23].

Assumption 3.1. The matrix $\mathbf{A} \in \mathbb{R}^{n \times n}$ in (1.1) is Hurwitz and $\|\mathcal{L}^{-1}\Pi\|_2 < 1$.

Remark 3.2. On first glance, the assumption $\|\mathcal{L}^{-1}\Pi\|_2 < 1$ sounds rather restrictive. Nevertheless, in the context of MOR, we can always proceed by defining the rescaled matrix

$$\tilde{\Pi} = \frac{1}{\|\mathcal{L}^{-1}\Pi\|_2 + \delta} \Pi,$$

for some $\delta > 0$ and observing that rescaling Π does not affect the space spanned by the columns of the solution matrix \mathbf{X} ; see [5, 9]. Since the columns space stays the same, the reachability and observability sets of the SLS are also correctly captured by the columns space of the solution of the rescaled system; see relation (2.3).

3.2. Error certification. An efficient implementation of [Algorithm 1](#) involves solving the following numerical issues:

- (i) At each iteration, the Lyapunov equation requires an efficient solver.
- (ii) An opportune stopping criterion is required for the stationary iterations.

In the following subsections, we describe how to address these points with a specific focus on the large-scale setting involving sparse matrices.

3.2.1. *Approximate solution of Lyapunov equations involving large sparse matrices.* Consider (3.2) with a large and sparse matrix \mathbf{A} . The literature for the case of large and sparse matrices is vast; see, for example, the survey [45] on methods for matrix equations and references therein. Almost all methods in the large-scale setting have in common that they construct a sequence of approximations that converge to the true solution. Thus, a suitable stopping criterion is required to balance the approximation error in the calculation of the solution of the Lyapunov equation and the solution of the stationary iteration from [Algorithm 1](#). To this end, assume that $\mathbf{X}_\ell \in \mathcal{S}_\geq^n$ is the approximation of the solution $\mathbf{X} \in \mathcal{S}_\geq^n$ of the Lyapunov equation (3.2) in the ℓ th step (and k th iteration of [Algorithm 1](#)) and let

$$\mathbf{R}_\ell := \mathbf{A}\mathbf{X}_\ell + \mathbf{X}_\ell\mathbf{A}^\top + \mathbf{B}_k\mathbf{B}_k^\top \quad (3.3)$$

denote the corresponding residual. We obtain the following error-residual relation.

Proposition 3.3 (Error bound for approximate solution of Lyapunov equations). *Consider the Lyapunov equation (3.2) with \mathbf{A} Hurwitz, and assume that $\mathbf{X}_\ell \in \mathcal{S}_\geq^n$ is an approximation of the unique solution $\mathbf{X} \in \mathcal{S}_\geq^n$ of (3.2). Let $\mathbf{E}_\ell := \mathbf{X}_\ell - \mathbf{X}$. Then*

$$\|\mathbf{E}_\ell\|_2 \leq \frac{\|\mathbf{R}_\ell\|_{\text{F}}}{2\sigma_{\min}(\mathbf{A})}, \quad (3.4)$$

where $\sigma_{\min}(\mathbf{A})$ denotes the smallest singular value of the matrix \mathbf{A} .

Proof. Substituting (3.2) into the residual equation (3.3) yields the error-residual relation

$$\mathbf{R}_\ell = \mathbf{A}\mathbf{E}_\ell + \mathbf{E}_\ell\mathbf{A}^\top, \quad (3.5)$$

which, together with the symmetry of \mathbf{R}_ℓ , yields that \mathbf{E}_ℓ is symmetric; see, e.g., [26, Cha. 12.3, Thm. 3]. Using Kronecker algebra and the notation introduced in (3.1) we can reformulate (3.5) in vectorial form as $\text{vec}(\mathbf{R}_\ell) = \mathcal{L} \text{vec}(\mathbf{E}_\ell)$. Using $\|\mathbf{E}\|_2 \leq \|\mathbf{E}\|_{\text{F}}$ and $\sigma_{\min}(\mathcal{L}) = 2\sigma_{\min}(\mathbf{A})$ yields

$$\begin{aligned} \|\mathbf{E}_\ell\|_2 &\leq \|\mathbf{E}_\ell\|_{\text{F}} = \|\text{vec}(\mathbf{E}_\ell)\|_2 = \|\mathcal{L}^{-1} \text{vec}(\mathbf{R}_\ell)\|_2 \leq \|\mathcal{L}^{-1}\|_2 \|\text{vec}(\mathbf{R}_\ell)\|_2 \\ &= \frac{\|\mathbf{R}_\ell\|_{\text{F}}}{\sigma_{\min}(\mathcal{L})} = \frac{\|\mathbf{R}_\ell\|_{\text{F}}}{2\sigma_{\min}(\mathbf{A})}. \end{aligned} \quad \square$$

We observe that the smallest singular value $\sigma_{\min}(\mathbf{A})$ needs to be computed only once. The computational cost is $\mathcal{O}(n)$ floating point operations if \mathbf{A} is sparse. In the large-scale case, one can, for example, rely on the method presented in [41]. The questions that remain to be answered are the following: (i) the choice of the iterative method to determine \mathbf{X}_ℓ and (ii) how to efficiently compute the residual norm $\|\mathbf{R}_\ell\|_{\text{F}}$. Since these questions are closely tied together, we first briefly describe the method for computing \mathbf{X}_ℓ . As proposed in [45], we project the Lyapunov equation (3.3) onto a smaller subspace and then use standard solvers for the small equation, thus obtaining the coordinates of the approximation in the subspace. We refer to [45, Sec. 5.1] for a review of the solution of small-scale Lyapunov equations.

More precisely, consider the matrix $\mathbf{V}_\ell \in \mathbb{R}^{n \times n_\ell}$ whose n_ℓ columns form an orthonormal basis of the appropriate subspace \mathcal{V}_ℓ that is to be used for the projection. Let $\mathbf{X}_\ell = \mathbf{V}_\ell \mathbf{Y}_\ell \mathbf{V}_\ell^\top$ be a low-rank approximation to the solution of (3.3) with $\mathbf{Y}_\ell \in \mathbb{R}^{n_\ell \times n_\ell}$. Imposing the Galerkin condition $\mathbf{V}_\ell^\top \mathbf{R}_\ell \mathbf{V}_\ell = \mathbf{0}$ on the residual, we obtain the lower-order projected Lyapunov equation

$$\mathbf{A}_\ell \mathbf{Y}_\ell + \mathbf{Y}_\ell \mathbf{A}_\ell^\top + \mathbf{B}_\ell \mathbf{B}_\ell^\top = \mathbf{0}, \quad (3.6)$$

with $\mathbf{A}_\ell := \mathbf{V}_\ell^\top \mathbf{A} \mathbf{V}_\ell$ and $\mathbf{B}_\ell := \mathbf{V}_\ell^\top \mathbf{B}_k$. For \mathcal{V}_ℓ , one can choose, for instance, the proposal from [36] and use the block Krylov subspace

$$\mathcal{K}_\ell(\mathbf{A}, \mathbf{B}_k) = \text{span}\{\mathbf{B}_k, \mathbf{A}\mathbf{B}_k, \mathbf{A}^2\mathbf{B}_k, \dots, \mathbf{A}^{\ell-1}\mathbf{B}_k\}. \quad (3.7)$$

For more sophisticated techniques, such as rational Krylov subspaces, we refer to [44, 45].

Besides computational efficiency, the low-rank approximation can also be exploited for an efficient evaluation of the Frobenius norm of the residual. Indeed, using the Krylov subspace (3.7), one can show $\|\mathbf{R}_\ell\| = \|\mathbf{V}_{\ell+1}^\top \mathbf{R}_\ell \mathbf{V}_{\ell+1}\|$ for the spectral and the Frobenius norm; see [44, Prop. 3.3]. This result is particularly convenient since, for $\mathbf{V}_{\ell+1} := [\mathbf{V}_\ell, \tilde{\mathbf{V}}]$, we have

$$\mathbf{V}_{\ell+1}^\top \mathbf{R}_\ell \mathbf{V}_{\ell+1} = \begin{bmatrix} \mathbf{V}_\ell^\top \mathbf{R}_\ell \mathbf{V}_\ell & \mathbf{V}_\ell^\top \mathbf{R}_\ell \tilde{\mathbf{V}} \\ \tilde{\mathbf{V}}^\top \mathbf{R}_\ell \mathbf{V}_\ell & \tilde{\mathbf{V}}^\top \mathbf{R}_\ell \tilde{\mathbf{V}} \end{bmatrix} = \begin{bmatrix} \mathbf{0} & \mathbf{Y}_\ell \mathbf{V}_\ell^\top \mathbf{A}^\top \tilde{\mathbf{V}} \\ \tilde{\mathbf{V}}^\top \mathbf{A} \mathbf{V}_\ell \mathbf{Y}_\ell & \mathbf{0} \end{bmatrix} \quad (3.8)$$

where we used the expression (3.3), the fact that $\mathbf{X}_\ell = \mathbf{V}_\ell \mathbf{Y}_\ell \mathbf{V}_\ell^\top$, and that $\tilde{\mathbf{V}}$ is, by construction, orthogonal to \mathbf{V}_ℓ and \mathbf{B}_k . From (3.8), it directly follows that

$$\|\mathbf{R}_\ell\|_{\text{F}} = \|\mathbf{V}_{\ell+1}^\top \mathbf{R}_\ell \mathbf{V}_{\ell+1}\|_{\text{F}} = 2\|\tilde{\mathbf{V}}^\top \mathbf{A} \mathbf{V}_\ell \mathbf{Y}_\ell\|_{\text{F}} \quad (3.9)$$

and the right hand side of (3.9) can be used to evaluate $\|\mathbf{R}_\ell\|_{\text{F}}$ in a computationally efficient way without the need to ever form the large-scale matrix \mathbf{R}_ℓ .

We conclude by observing that the use of the Krylov subspace (3.7) does not ensure that the residual decays monotonically over the iterations. However, there exist choices of subspaces, such as the one provided by *the generalized minimum residual* method, that can enforce monotonicity; see [22, Sec. 2.2].

3.2.2. Stopping criteria for Algorithm 1. Consider the approximate solution \mathbf{X}_k for the GLE (1.1) provided by Algorithm 1 at step k , and assume for the moment that the Lyapunov equation (3.2) is solved exactly. To understand whether such a solution is accurate enough for our requirements, we must estimate the norm of the approximation error.

Proposition 3.4 (Stopping criterion for Algorithm 1). *Suppose Assumption 3.1 is satisfied and consider the error $\mathbf{E}_k := \mathbf{X} - \mathbf{X}_k$, where \mathbf{X} is the unique solution of the GLE (1.1) and $\mathbf{X}_k = \mathbf{Z}_k \mathbf{Z}_k^\top$ is the unique solution of the Lyapunov equation (3.2) in iteration k of Algorithm 1. Then Algorithm 1 converges and*

$$\|\mathbf{E}_k\|_2 \leq \gamma \|\mathbf{X}_k - \mathbf{X}_{k-1}\|_{\text{F}}, \quad (3.10)$$

with

$$\gamma := \frac{\|\mathcal{L}^{-1} \Pi\|}{1 - \|\mathcal{L}^{-1} \Pi\|}. \quad (3.11)$$

Proof. Due to Algorithm 1 we obtain

$$\mathbf{A} \mathbf{X}_k + \mathbf{X}_k \mathbf{A}^\top + \sum_{j=1}^M \left(\mathbf{N}_j \mathbf{X}_{k-1} \mathbf{N}_j^\top \right) + \mathbf{B}_1 \mathbf{B}_1^\top = \mathbf{0} \quad (3.12)$$

for all $k \geq 2$. Then, from (1.1), we have $\mathbf{B}_1 \mathbf{B}_1^\top = -\mathbf{A} \mathbf{X} - \mathbf{X} \mathbf{A}^\top - \sum_{j=1}^M \left(\mathbf{N}_j \mathbf{X} \mathbf{N}_j^\top \right)$, and substituting into (3.12), we get

$$\mathbf{A} \mathbf{E}_k + \mathbf{E}_k \mathbf{A}^\top + \sum_{j=1}^M \left(\mathbf{N}_j \mathbf{E}_{k-1} \mathbf{N}_j^\top \right) = \mathbf{0}. \quad (3.13)$$

For convenience, we write (3.13) in its vectorial form $\mathcal{L} \operatorname{vec}(\mathbf{E}_k) = -\Pi \operatorname{vec}(\mathbf{E}_{k-1})$ with \mathcal{L} and Π defined in (3.1); thus, we have

$$\operatorname{vec}(\mathbf{E}_k) = -\mathcal{L}^{-1}\Pi \operatorname{vec}(\mathbf{E}_{k-1}). \quad (3.14)$$

Relation (3.14) directly implies that, from a numerical point of view, [Algorithm 1](#) converges, i.e., $\lim_{k \rightarrow \infty} \|\mathbf{E}_k\|_2 = 0$, if $\rho(\mathcal{L}^{-1}\Pi) < 1$, where $\rho(\mathcal{L}^{-1}\Pi)$ denotes the spectral radius of $\mathcal{L}^{-1}\Pi$; see also [10, 43]. Observe that $\mathbf{E}_{k-1} = \mathbf{E}_k + (\mathbf{X}_k - \mathbf{X}_{k-1})$, therefore, substituting in (3.14) and considering the norm on both sides, we get

$$\begin{aligned} \|\mathbf{E}_k\|_F &= \|\operatorname{vec}(\mathbf{E}_k)\|_2 = \|\mathcal{L}^{-1}\Pi \operatorname{vec}(\mathbf{E}_k + \mathbf{X}_k - \mathbf{X}_{k-1})\|_2 \\ &\leq \|\mathcal{L}^{-1}\Pi\|_2 (\|\mathbf{E}_k\|_F + \|\mathbf{X}_k - \mathbf{X}_{k-1}\|_F). \end{aligned}$$

By [Assumption 3.1](#), we have $\|\mathcal{L}^{-1}\Pi\| < 1$, and hence

$$\|\mathbf{E}_k\|_2 \leq \|\mathbf{E}_k\|_F \leq \frac{\|\mathcal{L}^{-1}\Pi\|_2}{1 - \|\mathcal{L}^{-1}\Pi\|_2} \|\mathbf{X}_k - \mathbf{X}_{k-1}\|_F. \quad \square$$

Last, we have to compute $\|\mathbf{X}_k - \mathbf{X}_{k-1}\|_F$, which would require $\mathcal{O}(n^2)$ floating point operations. To overcome this issue, we employ the following result.

Proposition 3.5. *Let $\mathbf{X}_k = \mathbf{Z}_k \mathbf{Z}_k^\top$ with $\mathbf{Z}_k \in \mathbb{R}^{n \times n_k}$ and $\mathbf{X}_{k-1} = \mathbf{Z}_{k-1} \mathbf{Z}_{k-1}^\top$ with $\mathbf{Z}_{k-1} \in \mathbb{R}^{n \times n_{k-1}}$ denote the respective solutions at iterations k and $k-1$ of [Algorithm 1](#). Without loss of generality assume $n_k = n_{k-1}$ ¹. Let*

$$\mathbf{X}_k = \mathbf{U}_k \boldsymbol{\Sigma}_k \mathbf{U}_k^\top, \quad \mathbf{X}_{k-1} = \mathbf{U}_{k-1} \boldsymbol{\Sigma}_{k-1} \mathbf{U}_{k-1}^\top,$$

denote the truncated eigenvalue decomposition for \mathbf{X}_k and \mathbf{X}_{k-1} , respectively, and assume

$$\mathbf{Z}_k = \mathbf{U}_k \boldsymbol{\Sigma}_k^{\frac{1}{2}}, \quad \mathbf{Z}_{k-1} = \mathbf{U}_{k-1} \boldsymbol{\Sigma}_{k-1}^{\frac{1}{2}}.$$

Then

$$\|\mathbf{X}_k - \mathbf{X}_{k-1}\|_F \leq \|(\mathbf{Z}_k - \mathbf{Z}_{k-1}) \boldsymbol{\Sigma}_k^{\frac{1}{2}}\|_F + \|(\mathbf{Z}_k - \mathbf{Z}_{k-1}) \boldsymbol{\Sigma}_{k-1}^{\frac{1}{2}}\|_F. \quad (3.15)$$

Proof. By making use of the triangular inequality it directly follows

$$\begin{aligned} \|\mathbf{X}_k - \mathbf{X}_{k-1}\|_F &= \|\mathbf{Z}_k \mathbf{Z}_k^\top - \mathbf{Z}_k \mathbf{Z}_{k-1}^\top + \mathbf{Z}_k \mathbf{Z}_{k-1}^\top - \mathbf{Z}_{k-1} \mathbf{Z}_{k-1}^\top\|_F \\ &\leq \|\mathbf{U}_k \boldsymbol{\Sigma}_k^{\frac{1}{2}} (\mathbf{Z}_k^\top - \mathbf{Z}_{k-1}^\top)\|_F + \|(\mathbf{Z}_k - \mathbf{Z}_{k-1}) \boldsymbol{\Sigma}_{k-1}^{\frac{1}{2}} \mathbf{U}_{k-1}^\top\|_F \\ &= \|(\mathbf{Z}_k - \mathbf{Z}_{k-1}) \boldsymbol{\Sigma}_k^{\frac{1}{2}}\|_F + \|(\mathbf{Z}_k - \mathbf{Z}_{k-1}) \boldsymbol{\Sigma}_{k-1}^{\frac{1}{2}}\|_F, \end{aligned}$$

where, for the last equality, we used the fact that \mathbf{U}_k and \mathbf{U}_{k-1} have orthonormal columns and that $\|\boldsymbol{\Sigma}_k^{\frac{1}{2}}(\mathbf{Z}_k - \mathbf{Z}_{k-1})\|_F = \|\boldsymbol{\Sigma}_k^{\frac{1}{2}}(\mathbf{Z}_k - \mathbf{Z}_{k-1})^\top\|_F$. \square

Replacing $\|\mathbf{X}_k - \mathbf{X}_{k-1}\|_F$ with the right-hand side of (3.15) has the advantage that we only need $\mathcal{O}(n)$ floating point operations for its evaluation (assuming $n_k, n_{k-1} \ll n$). With these preparations, we are now ready to formulate our main result for the approximate solution of [GLE](#) (1.1).

¹If this does not hold, it is enough to fill the $|n_k - n_{k-1}|$ missing columns of the smaller matrix with zero entries.

Theorem 3.6 (Error bound for the approximate solution of GLE). *Suppose Assumption 3.1 is satisfied. Let $\mathbf{X} = \mathbf{Z}\mathbf{Z}^\top$ with $\mathbf{Z} \in \mathbb{R}^{n \times n}$ be the unique solution of the GLE (1.1) and $\tilde{\mathbf{X}}_k = \tilde{\mathbf{Z}}_k \tilde{\mathbf{Z}}_k^\top$ with $\tilde{\mathbf{Z}}_k \in \mathbb{R}^{n \times n_k}$ be the approximate solution of the GLE computed at iteration k of Algorithm 1 applying the subspace projection method to solve the Lyapunov equation in (3.2). Then*

$$\|\mathbf{X} - \tilde{\mathbf{X}}_k\|_2 \leq \gamma \Delta_{k,k-1} + \frac{(1 + \gamma) \|\mathbf{R}_k\|_{\text{F}} + \gamma \|\mathbf{R}_{k-1}\|_{\text{F}}}{2\sigma_{\min}(\mathbf{A})}, \quad (3.16)$$

where \mathbf{R}_k and \mathbf{R}_{k-1} are the residuals corresponding to the approximation of the Lyapunov equation (3.2) at the k th and $(k-1)$ th iterations of Algorithm 1 due to the subspace approximation, respectively, γ is as defined in (3.11), and

$$\Delta_{k,k-1} := \|(\tilde{\mathbf{Z}}_k - \tilde{\mathbf{Z}}_{k-1})\tilde{\Sigma}_k^{\frac{1}{2}}\|_{\text{F}} + \|(\tilde{\mathbf{Z}}_k - \tilde{\mathbf{Z}}_{k-1})\tilde{\Sigma}_{k-1}^{\frac{1}{2}}\|_{\text{F}}. \quad (3.17)$$

Proof. Let \mathbf{X}_k be the exact solution of the Lyapunov equation (3.2) computed at step k of Algorithm 1. Using Propositions 3.3 and 3.4 we obtain

$$\|\mathbf{X} - \tilde{\mathbf{X}}_k\|_2 \leq \|\mathbf{X} - \mathbf{X}_k\|_2 + \|\mathbf{X}_k - \tilde{\mathbf{X}}_k\|_2 \leq \gamma \|\mathbf{X}_k - \mathbf{X}_{k-1}\|_{\text{F}} + \frac{\|\mathbf{R}_k\|_{\text{F}}}{2\sigma_{\min}(\mathbf{A})}. \quad (3.18)$$

Furthermore, the triangle inequality and Propositions 3.3 and 3.5 imply

$$\begin{aligned} \|\mathbf{X}_k - \mathbf{X}_{k-1}\|_{\text{F}} &\leq \|\mathbf{X}_k - \tilde{\mathbf{X}}_k\|_{\text{F}} + \|\tilde{\mathbf{X}}_k - \tilde{\mathbf{X}}_{k-1}\|_{\text{F}} + \|\tilde{\mathbf{X}}_{k-1} - \mathbf{X}_{k-1}\|_{\text{F}} \\ &\leq \frac{\|\mathbf{R}_k\|_{\text{F}}}{2\sigma_{\min}(\mathbf{A})} + \Delta_{k,k-1} + \frac{\|\mathbf{R}_{k-1}\|_{\text{F}}}{2\sigma_{\min}(\mathbf{A})}, \end{aligned}$$

yielding (3.16). \square

The practical use of (3.16) as a stopping criterion for Algorithm 1 requires the following clarifications.

(i) For the computation or approximation of $\|\mathcal{L}^{-1}\Pi\|_2$, we observe

$$\begin{aligned} \|\mathcal{L}^{-1}\Pi\|_2 &\leq \|\mathcal{L}^{-1}\|_2 \|\Pi\|_2 = \frac{1}{2\sigma_{\min}(\mathbf{A})} \left\| \sum_{j=1}^M \mathbf{N}_j \otimes \mathbf{N}_j \right\|_2 \\ &\leq \frac{1}{2\sigma_{\min}(\mathbf{A})} \sum_{j=1}^M \left\| \mathbf{N}_j \otimes \mathbf{N}_j \right\|_2 = \frac{1}{2\sigma_{\min}(\mathbf{A})} \sum_{j=1}^M \sigma_1(\mathbf{N}_j)^2, \end{aligned} \quad (3.19)$$

and (3.19) is computable in $\mathcal{O}(n)$ floating points operations if the involved matrices are sparse. This motivates, for any $\delta > 0$, to perform the scaling

$$\tilde{\mathbf{N}}_j := \frac{\mathbf{N}_j}{\sqrt{\beta + \delta}}, \quad \text{with} \quad \beta := \frac{1}{2\sigma_{\min}(\mathbf{A})} \sum_{j=1}^M \sigma_1(\mathbf{N}_j)^2, \quad j = 1, \dots, M; \quad (3.20)$$

see also Remark 3.2. Hence, it is not restrictive to consider $\gamma \approx 1$. Indeed, it is sufficient to scale (3.20) with $\delta = \beta$ to get $\gamma < 1$, and thus we can get rid of γ in (3.10).

(ii) Considering $\gamma = 1$, we can we require

$$\|\mathbf{R}_k\|_{\text{F}} \leq \zeta_1 \frac{2\sigma_{\min}(\mathbf{A})}{3} \text{tol}, \quad \Delta_{k,k-1} \leq \zeta_2 \text{tol}, \quad \text{with} \quad \zeta_1 + \zeta_2 = 1$$

during Algorithm 1 to obtain $\|\mathbf{X} - \mathbf{X}_k\|_2 \leq \text{tol}$. Our default choice is $\zeta_2 = 0.9$ and $\zeta_1 = 0.1$. Otherwise, a clever implementation consists of dynamically updating

the exit tolerance for the approximation of (3.2). For instance $\|\mathbf{R}_k\|_F \leq \text{tol}_{\text{Lyap},k}$ where

$$\text{tol}_{\text{Lyap},k} := \max \left\{ \zeta_1 2 \frac{\sigma_{\min}(\mathbf{A})}{3} \text{tol}, \min \left\{ \frac{\zeta_1}{\zeta_2} \Delta_{k-1,k-2}, \text{tol}_{\text{Lyap},k-1} \right\} \right\}$$

This allows us to save some computational effort since the accuracy for the resolution of the Lyapunov equation is scaled based on the current level of accuracy reached by the stationary iterations algorithm.

3.3. GLE error approximation and MOR. The error bound from [Theorem 2.4](#) relies on the singular values defined in (2.4) and on the LMIs (2.6). Both depend on the solution of the GLEs (2.2), which we can solve to a given tolerance using the results from the previous subsection. Nevertheless, [Theorem 2.4](#) relies on the exact Gramians, so it is fundamental to understand the impact of the numerical approximation error.

3.3.1. Preservation of LMIs for the approximated solution. After running algorithm [Algorithm 1](#) for k iterations, we obtain an approximate solution \mathbf{X}_k for the exact solution \mathbf{X} . The central problem we address is whether this approximation preserves the stability of the ROM and ensures that the error bound stated in [Theorem 2.4](#) remains valid. Specifically, even if the exact Gramians satisfy the LMIs in (2.7) and one of the LMIs in (2.6), there is no guaranty that the computed approximations will do the same. Therefore, we aim to establish conditions under which, if the exact Gramian \mathbf{X} (either the reachability Gramian satisfying (2.6a) or the controllability Gramian satisfying (2.6b)) fulfills the LMIs, then our approximation \mathbf{X}_k also does. This would guaranty the quadratic stability of the ROM and the applicability of [Theorem 2.4](#).

With this in mind, let us introduce the matrix $\hat{\mathbf{X}}$ that, under certain conditions on the \mathbf{A}_j matrices, satisfies the same LMIs as the exact solution \mathbf{X} . We construct $\hat{\mathbf{X}}$ using the approximation $\tilde{\mathbf{X}}$ given by [Algorithm 1](#) and leveraging [Theorem 3.6](#).

Theorem 3.7. *Suppose that the exact solution \mathbf{X} of (2.2a) satisfies the LMI (2.6a) and let $\tilde{\mathbf{X}}$ denote its approximation given by [Algorithm 1](#). Assume that the \mathbf{A}_j are dissipative, i.e.,*

$$\mathbf{A}_j + \mathbf{A}_j^\top \prec \mathbf{0}, \quad \text{for all } j \in \mathcal{J}. \quad (3.21)$$

Let $\mu \geq 0$ satisfy

$$\mu \geq \max_{j \in \mathcal{J}} \frac{\sigma_1(\mathbf{A}_j)}{\sigma_n(\mathbf{A}_j)} \|\mathbf{X} - \tilde{\mathbf{X}}\|_2 = \max_{j \in \mathcal{J}} \kappa(\mathbf{A}_j) \|\mathbf{X} - \tilde{\mathbf{X}}\|_2, \quad (3.22)$$

where $\kappa(\mathbf{A}_j)$ denotes the spectral condition number of \mathbf{A}_j . Then, the matrix

$$\hat{\mathbf{X}} := \tilde{\mathbf{X}} + \mu \mathbf{I}_n. \quad (3.23)$$

satisfies the LMI (2.6a).

Before proceeding with the proof of [Theorem 3.7](#), let us discuss the restriction on the type of SLS imposed by assumption (3.21). By the problem setup, we have that \mathbf{A}_j is Hurwitz; hence, it immediately follows that if \mathbf{A}_j is normal, i.e., $\mathbf{A}_j \mathbf{A}_j^* = \mathbf{A}_j^* \mathbf{A}_j$, then (3.21) holds since $\lambda_i(\mathbf{A}_j + \mathbf{A}_j^\top) = 2 \operatorname{Re}(\lambda_i(\mathbf{A}_j))$. Also, it is not difficult to show that every real Hurwitz matrix can be factorized as

$$\mathbf{A}_j = (\mathbf{J}_j - \mathbf{R}_j) \mathbf{Q}_j, \quad (3.24)$$

with $\mathbf{J}_j \in \mathbb{R}^{n \times n}$ skew-symmetric, $\mathbf{R}_j \in \mathbb{R}^{n \times n}$ symmetric positive semi-definite, and $\mathbf{Q}_j \in \mathbb{R}^{n \times n}$ symmetric positive definite; cf. [14]. Whenever $\mathbf{Q}_j = \mathbf{I}_n$ for all $j \in \mathcal{J}$, it is straightforward to check that (3.21) is verified. Moreover, if the SLS is quadratically stable, then there exists a symmetric positive-definite \mathbf{Q} such that one can choose $\mathbf{Q}_j = \mathbf{Q}$ for all $j \in \mathcal{J}$ in (3.24), such that (3.21) is satisfied after a suitable coordinate transformation; see [40].

Proof of Theorem 3.7. By the assumptions, \mathbf{X} satisfies the LMIs

$$\mathbf{A}_j \mathbf{X} + \mathbf{X} \mathbf{A}_j^\top + \mathbf{B}_j \mathbf{B}_j^\top \prec \mathbf{0} \quad \text{for all } j \in \mathcal{J}, \quad (3.25)$$

and we need to show that

$$\mathbf{w}^\top (\mathbf{A}_j \hat{\mathbf{X}} + \hat{\mathbf{X}} \mathbf{A}_j^\top + \mathbf{B}_j \mathbf{B}_j^\top) \mathbf{w} < \mathbf{0} \quad \text{for all } j \in \mathcal{J} \text{ and for all } \mathbf{w} \in \mathbb{R}^n \setminus \{\mathbf{0}\}. \quad (3.26)$$

Using (3.25), we observe $\mathbf{w}^\top \mathbf{B}_j \mathbf{B}_j^\top \mathbf{w} < -2\mathbf{w}^\top \mathbf{X} \mathbf{A}_j^\top \mathbf{w}$. Substituting into (3.26) yields

$$2\mathbf{w}^\top \hat{\mathbf{X}} \mathbf{A}_j^\top \mathbf{w} + \mathbf{w}^\top \mathbf{B}_j \mathbf{B}_j^\top \mathbf{w} < 2\mathbf{w}^\top \hat{\mathbf{E}} \mathbf{A}_j^\top \mathbf{w} \quad (3.27)$$

with $\hat{\mathbf{E}} := \hat{\mathbf{X}} - \mathbf{X}$. Defining $\tilde{\mathbf{E}} := \tilde{\mathbf{X}} - \mathbf{X}$ and using (3.23) implies

$$\mathbf{w}^\top \hat{\mathbf{E}} \mathbf{A}_j^\top \mathbf{w} = \mathbf{w}^\top \tilde{\mathbf{E}} \mathbf{A}_j^\top \mathbf{w} + \mu \mathbf{w}^\top \mathbf{A}_j^\top \mathbf{w} \leq \|\mathbf{w}\|_2^2 (\sigma_1(\mathbf{A}_j) \|\tilde{\mathbf{E}}\|_2 - \sigma_n(\mathbf{A}_j) \mu),$$

where we used the fact that $\mathbf{w}^\top \mathbf{A}_j^\top \mathbf{w} < 0$ for all $\mathbf{w} \in \mathbb{R}^n \setminus \{\mathbf{0}\}$ due to (3.21). The result thus follows immediately from (3.22). \square

Remark 3.8. The statement of Theorem 3.7 can also be formulated in terms of the observability Gramian, in which case we need to assume that the LMIs (2.6b) are satisfied. The proof is analogously to the proof above.

Therefore, if we compute $\tilde{\mathbf{X}}$ such that $\|\mathbf{X} - \tilde{\mathbf{X}}\|_2 \leq \text{tol}$, then we can choose

$$\mu = \hat{\mu} := \text{tol} \max_{j=1,\dots,M} \kappa(\mathbf{A}_j) \quad (3.28)$$

to enforce the LMIs for the approximated solution. However, for large-scale systems arising from some PDE discretization, $\kappa(\mathbf{A}_j)$ may be large, resulting in μ several orders of magnitude larger than tol . In this way, the sum of the neglected singular values of $\hat{\mathbf{X}}$ can't be less than μ , dramatically affecting the sharpness of the error estimate (2.8).

4. MOR FOR SLS USING PIECEWISE CONSTANT GRAMIANS

The main challenge in MOR for SLS based on approximate GLE solutions is to ensure both the stability of the ROM and the validity of the error bound from Theorem 2.4. Achieving this requires that the solutions of the GLEs in (2.2) satisfy the LMIs (2.6). For a specific class of SLS, Theorem 3.7 provides a way to perturb an approximate GLE solution so that the resulting perturbed solution satisfies the LMIs, assuming the exact solution does as well. However, the condition in (3.28) within Theorem 3.7 can reduce the sharpness of the error bound and applies only to SLS that satisfy (3.21). Furthermore, it may not always be clear whether the exact solutions of the GLEs satisfy the LMIs in the first place. To overcome these limitations, we propose a novel MOR strategy for SLS that guarantees the stability of the ROM and provides a generalized error bound without requiring the LMIs to hold.

4.1. Piecewise balancing reduction for SLS. We start with the observation that if in (2.2a) we set $\mathbf{A} = \mathbf{A}_j$, then it is straightforward to see that the GLE solution satisfies the LMI

$$\mathbf{A}_j \mathbf{X} + \mathbf{X} \mathbf{A}_j^\top + \mathbf{B}_j \mathbf{B}_j \preceq 0. \quad (4.1)$$

Therefore, each exact solution of the GLE with $\mathbf{A} = \mathbf{A}_j$ always satisfies at least the LMI (4.1). This inspires the following idea: for each $j \in \mathcal{J}$, solve the GLE with $\mathbf{A} = \mathbf{A}_j$ (and correspondingly updated \mathbf{N}_i) and, following the MOR procedure described in Section 2.2, compute the projection matrices (2.5), which we denote as \mathbf{V}_j and \mathbf{W}_j to highlight that they originate from the GLE where $\mathbf{A} = \mathbf{A}_j$. Then, we introduce the following reduced systems with state transition matrices

$$\hat{\Sigma}_q \quad \left\{ \begin{array}{l} \dot{\tilde{\mathbf{x}}}(t) = \hat{\mathbf{A}}_{q(t)} \tilde{\mathbf{x}}(t) + \hat{\mathbf{B}}_{q(t)} \mathbf{u}(t), \quad \tilde{\mathbf{x}}(t_0) = \mathbf{0}, \\ \tilde{\mathbf{x}}(t_k^+) = \mathbf{W}_{q_k}^\top \mathbf{V}_{q_{k-1}} \tilde{\mathbf{x}}(t_k^-), \\ \tilde{\mathbf{y}}(t) = \hat{\mathbf{C}}_{q(t)} \tilde{\mathbf{x}}(t), \end{array} \right. \quad (4.2)$$

where t_k are the switching times for the particular $q \in \mathcal{S}$, $q_k := q(t_k)$, and

$$\hat{\mathbf{A}}_j := \mathbf{W}_j^\top \mathbf{A}_j \mathbf{V}_j \in \mathbb{R}^{r_j \times r_j}, \quad \hat{\mathbf{B}}_j := \mathbf{W}_j^\top \mathbf{B}_j \in \mathbb{R}^{r_j \times m}, \quad \hat{\mathbf{C}}_j := \mathbf{C}_j \mathbf{V}_j \in \mathbb{R}^{p \times r_j} \quad (4.3)$$

for $j \in \mathcal{J}$. We call this procedure the *piecewise balancing reduction* (PBR) for SLS. In the next sections, we discuss the stability of the reduced SLS (4.2).

4.2. Stability of the PBR for SLS. We start with the following proposition.

Proposition 4.1. *Assume that the GLEs (2.2) are solved exactly with $\mathbf{A} = \mathbf{A}_j$ and correspondingly updated \mathbf{N}_i for $i, j \in \mathcal{J}$. Then, each subsystem of the switched system $\hat{\Sigma}_q$ defined in (4.2) is stable.*

Proof. The stability arises from the observation that the solutions \mathcal{P}_j and \mathcal{Q}_j of GLEs can be interpreted as generalized Gramians for the mode j of the SLS; see [13, Sec. 4.7]. Therefore, each $\hat{\mathbf{A}}_j$ is, by construction, stable due to the stability properties of classical square root balance truncation. \square

As already discussed in Section 2.2, the fact that each subsystem mode is stable is not sufficient to conclude that the SLS is stable for each $q \in \mathcal{S}$. However, having stable subsystems represents an improvement over what the reduction procedure described in Section 2.2 can achieve. Indeed, for that strategy, stable subsystems cannot be guaranteed if at least one of the LMIs in (2.6) is not satisfied by one of the exact solutions of (2.2).

To further investigate the stability of (4.2), one can attempt to solve the following set of LMI

$$\hat{\mathbf{A}}_j^\top \hat{\mathbf{P}} + \hat{\mathbf{P}} \hat{\mathbf{A}}_j \prec \mathbf{0}, \quad \text{for all } j \in \mathcal{J}$$

to verify the quadratic stability property. Since the SLS is now of size $r \ll n$, solving the LMI is a much cheaper computational task. Moreover, if the solution of the LMI is not successful, it is possible to exploit the fact that the asymptotic stability of the SLS can still be guaranteed under a minimum switching time condition; see [28, Sec. 3.2.1].

4.3. Accuracy of the PBR for SLS. To obtain an error bound for the PBR, we will rely on standard techniques used to derive the classical balanced truncation error estimate. In particular, we start by first investigating the effect of truncation only the smallest singular value, see the forthcoming [Lemma 4.2](#), and then iteratively apply this result to obtain the error bound, which we present in the forthcoming [Theorem 4.3](#). In contrast to the classical setting, however, we must take into consideration that the Gramians are time-dependent (piecewise constant in time) and the possibility that the LMI s may not be exactly satisfied. Let us start by defining the following piecewise constant matrices

$$\tilde{\mathcal{P}}(t) := \tilde{\mathcal{P}}_{q(t)}, \quad \tilde{\mathcal{Q}}(t) := \tilde{\mathcal{Q}}_{q(t)}, \quad (4.4)$$

where $\tilde{\mathcal{P}}_j$ and $\tilde{\mathcal{Q}}_j$ are the approximated solutions of [\(2.2a\)](#) and [\(2.2b\)](#), respectively, for $\mathbf{A} = \mathbf{A}_j$ obtained via [Algorithm 1](#). Then, for each $j \in \mathcal{J}$, consider the factorizations $\tilde{\mathcal{P}}_j = \tilde{\mathbf{S}}_j \tilde{\mathbf{S}}_j^\top$, $\tilde{\mathcal{Q}}_j = \tilde{\mathbf{R}}_j \tilde{\mathbf{R}}_j^\top$, and $\tilde{\mathbf{S}}_j^\top \tilde{\mathbf{R}}_j = \mathbf{U}_j \Sigma_j \mathbf{V}_j^\top$. The transformations to balance mode j are given by

$$\bar{\mathbf{V}}_j := \tilde{\mathbf{S}}_j \mathbf{U}_j \Sigma_j^{-1/2} \quad \text{and} \quad \bar{\mathbf{W}}_j := \tilde{\mathbf{R}}_j \mathbf{V}_j \Sigma_j^{-1/2} = \bar{\mathbf{V}}_j^{-\top}.$$

Balancing each mode of system [\(1.2\)](#) and performing the truncation, we get the SLS [\(4.2\)](#) with state transitions. For a switching signal $q \in \mathcal{S}$, let us introduce the set of switching times up to time t , which we denote as $\mathcal{T}_{q(t)} := \{t_1, \dots, t_K\}$, with $K \in \mathbb{N}$. Now, let us suppose that each subsystem j of the SLS in [\(1.2\)](#) is balanced via $\tilde{\mathcal{P}}_j$ and $\tilde{\mathcal{Q}}_j$; thus, the generalized observability and controllability Gramians are of the form

$$\Sigma_j = \begin{bmatrix} \Sigma_{j,1} & \mathbf{0} \\ \mathbf{0} & \sigma(j) \mathbf{I}_{m(j)} \end{bmatrix} \quad \text{with} \quad \Sigma_{j,1} \in \mathbb{R}^{(n-m(j)) \times (n-m(j))} \quad (4.5)$$

where $m(j)$ is the multiplicity of $\sigma(j)$ implying that $\sigma(j) \notin \Sigma_{j,i}$. For simplicity, let us assume $\tilde{m} = m(j)$ for all $j \in \mathcal{J}$ (similar results can be stated without considering the minimum value of the multiplicity among the M system modes). Because of [\(4.5\)](#), it is convenient for us to rewrite the system matrices \mathbf{A}_j , \mathbf{B}_j , and \mathbf{C}_j for each $j \in \mathcal{J}$ in their balanced form

$$\bar{\mathbf{A}}_j := \begin{bmatrix} \hat{\mathbf{A}}_j & \mathbf{A}_{j,12} \\ \mathbf{A}_{j,21} & \mathbf{A}_{j,22} \end{bmatrix}, \quad \bar{\mathbf{B}}_j := \begin{bmatrix} \hat{\mathbf{B}}_j \\ \mathbf{B}_{j,2} \end{bmatrix}, \quad \bar{\mathbf{C}}_j := \begin{bmatrix} \hat{\mathbf{C}}_j & \mathbf{C}_{j,2} \end{bmatrix}, \quad (4.6)$$

where $\hat{\mathbf{A}}_j$, $\hat{\mathbf{B}}_j$, and $\hat{\mathbf{C}}_j$ is the j subsystem of [\(4.2\)](#) with $r = n - \tilde{m}$.

Lemma 4.2. *Consider the ROM [\(4.2\)](#) for $r = n - \tilde{m}$ and the FOM in balanced form [\(4.6\)](#). Take the decomposition $\bar{\mathbf{x}}(t) = [\bar{\mathbf{x}}_1(t)^\top, \bar{\mathbf{x}}_2(t)^\top]^\top$ where $\bar{\mathbf{x}}_1(t) \in \mathbb{R}^r$ and let us define the vectors*

$$\mathbf{x}_c(t) := \begin{bmatrix} \bar{\mathbf{x}}_1(t) + \tilde{\mathbf{x}}(t) \\ \bar{\mathbf{x}}_2(t) \end{bmatrix} \quad \text{and} \quad \mathbf{x}_o(t) := \begin{bmatrix} \bar{\mathbf{x}}_1(t) - \tilde{\mathbf{x}}(t) \\ \bar{\mathbf{x}}_2(t) \end{bmatrix}. \quad (4.7)$$

For given $q \in \mathcal{S}$ with switching times t_k ($k = 1, \dots, K$), we introduce the quantities

$$\begin{aligned}
\mathcal{G}_{o,q}(n, r) &:= \mathbf{x}_o^\top(t) \boldsymbol{\Sigma}_{q(t)} \mathbf{x}_o(t) + \sum_{k=1}^K \left(\mathbf{x}_o^\top(t_k^-) \boldsymbol{\Sigma}_{q(t_k^-)} \mathbf{x}_o(t_k^-) - \mathbf{x}_o^\top(t_k^+) \boldsymbol{\Sigma}_{q(t_k^+)} \mathbf{x}_o(t_k^+) \right), \\
\mathcal{G}_{c,q}(n, r) &:= \sigma(q(t_K^+))^2 \mathbf{x}_c^\top(t) \boldsymbol{\Sigma}_{q(t)}^{-1} \mathbf{x}_c(t) \\
&\quad + \sum_{k=1}^K \left(\sigma(q(t_k^-))^2 \mathbf{x}_c^\top(t_k^-) \boldsymbol{\Sigma}_{q(t_k^-)}^{-1} \mathbf{x}_c(t_k^-) - \sigma(q(t_k^+))^2 \mathbf{x}_c^\top(t_k^+) \boldsymbol{\Sigma}_{q(t_k^+)}^{-1} \mathbf{x}_c(t_k^+) \right), \\
\mathbf{M}_c(j) &:= \bar{\mathbf{A}}_j \Sigma_j + \Sigma_j \bar{\mathbf{A}}_j^\top + \bar{\mathbf{B}}_j \bar{\mathbf{B}}_j^\top, \quad \mathbf{M}_o(j) := \bar{\mathbf{A}}_j^\top \Sigma_j + \Sigma_j \bar{\mathbf{A}}_j^\top + \bar{\mathbf{C}}_j \bar{\mathbf{C}}_j^\top, \\
\mathcal{H}_{c,q}(n, r) &:= \sum_{k=0}^K \lambda_1(\mathbf{M}_c(q(t_k^+))) \int_{t_k}^{t_{k+1}} \|\mathbf{x}_c(s)\|_2^2 \, ds, \\
\mathcal{H}_{o,q}(n, r) &:= \sum_{k=0}^K \lambda_1(\mathbf{M}_o(q(t_k^+))) \int_{t_k}^{t_{k+1}} \|\mathbf{x}_o(s)\|_2^2 \, ds.
\end{aligned} \tag{4.8}$$

Then, the output between the FOM (1.2) and the ROM (4.2) of size $r = n - \tilde{m}$ satisfies the relation

$$\begin{aligned}
\left(\int_0^t \|\mathbf{y}(s) - \tilde{\mathbf{y}}(s)\|_2^2 \, ds \right)^{\frac{1}{2}} &\leq \left(\mathcal{H}_{c,q}(n, r) + \mathcal{H}_{o,q}(n, r) - (\mathcal{G}_{o,q}(n, r) + \mathcal{G}_{c,q}(n, r)) \right. \\
&\quad \left. + 4\tilde{\sigma}^2 \int_0^t \|\mathbf{u}(s)\|_2^2 \, ds \right)^{\frac{1}{2}},
\end{aligned} \tag{4.9}$$

with $\tilde{\sigma} := \max_{j=1, \dots, M} \sigma(j)$

Proof. The proof is provided in [Appendix A.1](#). It follows the steps of [\[34, Lem. 13\]](#) and [\[37\]](#), although these references do not consider piecewise Gramians and assume that the LMI are satisfied. \square

Before iteratively applying [Lemma 4.2](#) to obtain the error bound, let us introduce and comment on some notations. Given $r \ll n$ and $k \in \mathbb{N}$ with $k > r$, we denote the distinct singular values of the balanced Gramian (4.5) and their associated multiplicities by $\sigma_k(j)$ and $m_k(j)$, for $k = r + 1, \dots, \tilde{n}$, respectively. In order to simplify the notation, we impose the assumption that $m_k(j_1) = m_k(j_2)$ holds for all $j_1, j_2 \in \mathcal{J}$ and for all $k = r + 1, \dots, \tilde{n}$. This allows dropping the j dependence for $m_k(j)$ and avoids the introduction of additional heavy notation in the statement of the next theorem. In general, we could state the next results without distinguishing between simple and non-simple singular values. However, as we will comment later, it is crucial to deal with the case where the smallest singular value of the Gramian (4.5) is not simple, as this allows for a sharper error bound that is also efficiently computable.

Theorem 4.3 (Error bound of the PBR for SLS). *Given a switching signal $q \in \mathcal{S}$, consider the ROM (4.2) of size r . Then, the output error between the FOM (1.2) and the ROM (4.2)*

of size r satisfies the relation

$$\begin{aligned} \left(\int_0^t \|\mathbf{y}(s) - \tilde{\mathbf{y}}(s)\|_2^2 ds \right)^{\frac{1}{2}} &\leq 2 \left(\int_0^t \|\mathbf{u}(s)\|_2^2 ds \right)^{\frac{1}{2}} \sum_{k=r+1}^{\tilde{n}} \tilde{\sigma}_{s_k} \\ &+ \sum_{k=r+1}^{\tilde{n}} \mathcal{H}_{c,o,q}(s_{k+1}, s_k)^{\frac{1}{2}} H(\mathcal{H}_{c,o,q}(s_{k+1}, s_k)) \\ &- \sum_{k=r+1}^{\tilde{n}} \mathcal{G}_{c,o,q}(s_{k+1}, s_k)^{\frac{1}{2}} H(-\mathcal{G}_{c,o,q}(s_{k+1}, s_k)), \end{aligned} \quad (4.10)$$

where $H(x)$ is the Heaviside function, $\tilde{\sigma}_k := \max_{j \in \mathcal{J}} \sigma_k(j)$, $s_k := \sum_{k=r}^{\tilde{n}} m_k$, $m_r := r$, and

$$\begin{aligned} \mathcal{H}_{c,o,q}(s_{k+1}, s_k) &:= \mathcal{H}_{o,q}(s_{k+1}, s_k) + \mathcal{H}_{c,q}(s_{k+1}, s_k), \\ \mathcal{G}_{c,o,q}(s_{k+1}, s_k) &:= \mathcal{G}_{o,q}(s_{k+1}, s_k) + \mathcal{G}_{c,q}(s_{k+1}, s_k). \end{aligned}$$

Proof. The proof follows directly by applying the sub-additivity of the square root function to [Lemma 4.2](#) and standard balance truncation error arguments; see, for instance, [34, Sec. 7]. \square

The error bound presented in [Theorem 4.3](#) comprises three distinct contributions: the first corresponds to the sum of the truncated singular values, as in [Theorem 2.4](#); the second stems from the use of piecewise constant Gramians in the derivation of (4.2); and the third reflects the fact that the numerically computed solutions of the GLE may not exactly satisfy the LMI conditions due to approximation errors. In this regard, [Theorem 4.3](#) extends [Theorem 2.4](#) by incorporating the effects of piecewise constant Gramians and not requiring that the LMI conditions are fulfilled exactly. However, this generalization comes at the cost of requiring the reduced state trajectory to be computed in order to evaluate the error bound. This a-posteriori evaluation step is not required for the bound in [Theorem 2.4](#).

Remark 4.4. *The proof of [Lemma 4.2](#) requires (4.5) to be invertible. To maintain computational efficiency, we apply truncation when computing the approximate GLE solution $\tilde{\mathbf{X}}$, i.e., we discard all singular values smaller than the prescribed accuracy threshold tol . As a result, (4.5) becomes singular once the reduced dimension is sufficiently large. To address this, we replace the zero singular values with tol , thereby ensuring that (4.5) remains invertible. Moreover, in terms of the error estimates, since we are introducing non-simple singular values, we only need to take them into account once in the error estimate (4.3). In practice, this is done by adding tol to each of the diagonal entries of Σ_j for $j = 1, \dots, M$.*

4.4. Tightening the error bound. In the following, we propose a methodology to make tighten the error bound (4.10) by enforcing non-positivity of the eigenvalues of $\mathbf{M}_c(j)$ (and $\mathbf{M}_o(j)$) by suitably perturbing $\tilde{\mathbf{X}}_j$. Plugging $\tilde{\mathbf{X}}_j$ into the GLE for $\mathbf{A} = \mathbf{A}_j$ with correspondingly upgrated \mathbf{N}_j , we can define the j -th residual

$$\tilde{\mathbf{R}}_j := \mathbf{A}_j \tilde{\mathbf{X}}_j + \tilde{\mathbf{X}}_j \mathbf{A}_j^\top + \sum_{i=1}^M \left(\mathbf{N}_i \tilde{\mathbf{X}}_j \mathbf{N}_i^\top + \mathbf{B}_i \mathbf{B}_i^\top \right).$$

The matrix $\tilde{\mathbf{R}}_j$ is symmetric and, in general, indefinite. Let us write its eigenvalue decomposition as

$$\tilde{\mathbf{R}}_j = [\mathbf{V}_j^- \ \mathbf{V}_j^+] \begin{bmatrix} \Sigma_j^- & \mathbf{0} \\ \mathbf{0} & \Sigma_j^+ \end{bmatrix} [\mathbf{V}_j^- \ \mathbf{V}_j^+]^\top, \quad (4.11)$$

where Σ_j^- , Σ_j^+ are the diagonal matrices containing the non-positive and the positive eigenvalues, respectively, while the columns of the matrices \mathbf{V}_j^- , \mathbf{V}_j^+ are the associated orthonormal eigenvectors. We now define Δ_j as the solution to the Lyapunov equation

$$\mathbf{A}_j \Delta_j + \Delta_j \mathbf{A}_j^\top + \mathbf{V}_j^+ \Sigma_j^+ (\mathbf{V}_j^+)^{\top} = \mathbf{0}. \quad (4.12)$$

Proposition 4.5. *The matrix $\hat{\mathbf{X}}_j := \tilde{\mathbf{X}}_j + \Delta_j$ with Δ_j being the unique solution of (4.12) satisfies*

$$\mathbf{A}_j \hat{\mathbf{X}}_j + \hat{\mathbf{X}}_j \mathbf{A}_j^\top + \mathbf{B}_j \mathbf{B}_j^\top \preceq \mathbf{0}.$$

Proof. We have

$$\begin{aligned} \mathbf{A}_j \hat{\mathbf{X}}_j + \hat{\mathbf{X}}_j \mathbf{A}_j^\top + \mathbf{B}_j \mathbf{B}_j^\top &\preceq \mathbf{A}_j \hat{\mathbf{X}}_j + \hat{\mathbf{X}}_j \mathbf{A}_j^\top + \sum_{i=1}^M \left(\mathbf{N}_i \tilde{\mathbf{X}}_j \mathbf{N}_i^\top + \mathbf{B}_i \mathbf{B}_i^\top \right) \\ &= \tilde{\mathbf{R}}_j + \mathbf{A}_j \Delta_j + \Delta_j \mathbf{A}_j^\top = \mathbf{V}_j^- \Sigma_j^- (\mathbf{V}_j^-)^\top \preceq \mathbf{0}, \end{aligned}$$

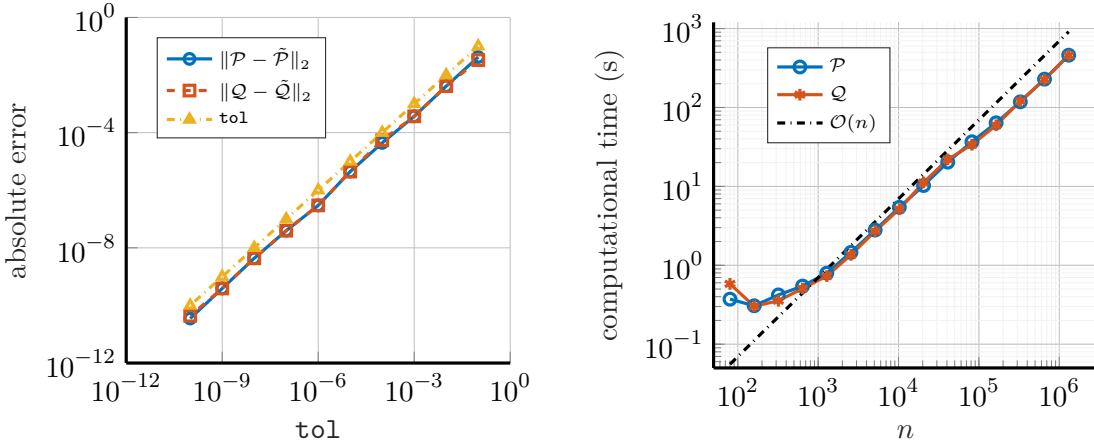
where we used (4.12) and (4.11). \square

4.5. Numerical aspects concerning Sections 4.3 and 4.4. We start detailing how the numerics involved in computing and storing $\hat{\mathbf{X}}_j$ can be performed efficiently.

- (i) For any $j \in \mathcal{J}$, we need to compute the positive eigenvalues and associated eigenvectors of $\tilde{\mathbf{R}}_j$. Their computation can be performed without explicitly forming $\tilde{\mathbf{R}}_j$, exploiting the low-rank factor $\tilde{\mathbf{Z}}_j$ of $\tilde{\mathbf{X}}_j$ and employing only matrix-vector products; see [27].
- (ii) For each $j \in \mathcal{J}$, our method requires solving the Lyapunov equation (4.12) in addition to using Algorithm 1 to compute $\hat{\mathbf{X}}_j$. Solving Lyapunov equations still introduces numerical errors; however, being a simpler matrix equation than the GLE, we can solve it with higher accuracy without compromising the overall computational cost.
- (iii) The evaluation of Δ_j is more efficient as fewer positive eigenvalues are present in $\tilde{\mathbf{R}}_j$ for all $j \in \mathcal{J}$. Their number may not be small in general; however, even computing a few of the largest ones is enough to tighten the error bound and improve the accuracy of the ROM.
- (iv) We do not explicitly compute Δ_j , but rather compute an approximation $\tilde{\Delta}_j$ by storing its low-rank factor, say $\tilde{\mathbf{G}}_j$, such that $\tilde{\Delta}_j = \tilde{\mathbf{G}}_j \tilde{\mathbf{G}}_j^\top$. In particular, (4.12) must be solved with significantly higher accuracy than the corresponding GLE. To form $\hat{\mathbf{X}}_j$, we append the low rank factors of $\tilde{\Delta}_j$ to those of $\tilde{\mathbf{X}}_j$, i.e.,

$$\hat{\mathbf{X}}_j = [\tilde{\mathbf{Z}}_j \ \tilde{\mathbf{G}}_j] [\tilde{\mathbf{Z}}_j \ \tilde{\mathbf{G}}_j]^\top. \quad (4.13)$$

We conclude by commenting on the error bound of Theorem 4.3. Evaluating Theorem 4.3 requires computing all reduced state trajectories from dimension r to n , which is computationally inefficient. However, since the reduced system is in a balanced form, the entries of the state decay rapidly. Therefore, it is reasonable to approximate the reduced state at



(a) Absolute error vs. exit tolerance tol for the computing the Gramians with [Algorithm 1](#) for $n = 200$.

(b) Computational time to solve the GLEs with respect to the size of the full problem n .

Figure 1 – Synthetic example (5.1).

higher dimensions using the trajectory computed at a smaller dimension—provided that the last reduced state components are significantly smaller than the target accuracy.

5. NUMERICAL EXPERIMENTS

In this section, we present numerical experiments to support both the theoretical results and the proposed methodology. We begin by validating the theory developed in [Section 3](#) using a synthetic example from [\[35, Sec. V\]](#). Subsequently, we illustrate the theoretical framework of [Section 4](#) through a test case based on the parametric Black–Scholes model, where switching behavior is induced by treating the parameter as piecewise constant in time. All calculations were performed with MATLAB 2024b on a laptop with an Apple M2 Pro processor and 16GB of RAM.

The code and data used to generate the subsequent results are accessible via

<https://doi.org/10.5281/zenodo.17880696>

under MIT Common License.

5.1. Synthetic example. Let us consider a 2-mode switched linear system of dimension n , with state matrices given by $\mathbf{A}_1, \mathbf{A}_2 \in \mathbb{R}^{n \times n}$ such that

$$\mathbf{A}_1(i, j) := \begin{cases} -1, & \text{if } i = j \\ \frac{1}{2}, & \text{if } i - 1 = j \\ 0, & \text{otherwise} \end{cases}, \quad \mathbf{A}_2(i, j) := \begin{cases} -2, & \text{if } i = j \\ \frac{4}{5}, & \text{if } i - 1 = j \\ -\frac{1}{5}, & \text{if } i + 1 = j \\ 0, & \text{elsewhere} \end{cases} \quad (5.1)$$

and $\mathbf{B}_1^\top = \mathbf{C}_1 = [0, \dots, 0, 1]$, $\mathbf{B}_2^\top = \mathbf{C}_2 = [1, 0, \dots, 0]$. We set $\mathbf{A} = \mathbf{A}_1$, $\mathbf{N}_1 = \mathbf{0}$, and $\mathbf{N}_2 = \mathbf{A}_2 - \mathbf{A}_1$ to obtain the GLE setting in [\(1.1\)](#).

In our first experiment, we set $n = 200$ and we compare the approximate Gramians computed via [Algorithm 1](#) against the exact ones obtained by solving the full $n^2 \times n^2$ linear

tol	$\hat{\mu}$	$\lambda_1(\mathcal{M}_1(\tilde{\mathcal{P}}))$	$\lambda_1(\mathcal{M}_1(\hat{\mathcal{P}}))$	$\lambda_1(\mathcal{M}_2(\tilde{\mathcal{P}}))$	$\lambda_1(\mathcal{M}_2(\hat{\mathcal{P}}))$
10^{-2}	$3.0 \cdot 10^{-2}$	$1.0 \cdot 10^{-3}$	$-3.0 \cdot 10^{-2}$	$1.2 \cdot 10^{-3}$	$-8.4 \cdot 10^{-2}$
10^{-4}	$3.0 \cdot 10^{-4}$	$1.6 \cdot 10^{-5}$	$-3.0 \cdot 10^{-4}$	$7.6 \cdot 10^{-6}$	$-8.4 \cdot 10^{-4}$
10^{-6}	$3.0 \cdot 10^{-6}$	$3.8 \cdot 10^{-8}$	$-3.0 \cdot 10^{-6}$	$4.8 \cdot 10^{-8}$	$-8.4 \cdot 10^{-6}$
10^{-8}	$3.0 \cdot 10^{-8}$	$1.3 \cdot 10^{-9}$	$-3.0 \cdot 10^{-8}$	$1.7 \cdot 10^{-9}$	$-8.4 \cdot 10^{-8}$
10^{-10}	$3.0 \cdot 10^{-10}$	$8.6 \cdot 10^{-12}$	$-3.0 \cdot 10^{-10}$	$1.1 \cdot 10^{-11}$	$-8.4 \cdot 10^{-10}$

Table 1 – Synthetic example (5.1) for $n = 200$. The table reports the values of $\hat{\mu}$ (as defined in (3.28)) and the satisfaction of the LMIs in (2.6a) for both the approximated Gramian $\tilde{\mathcal{P}}$ and the generalized Gramian $\hat{\mathcal{P}}$, across different values of the approximation tolerance `tol` used in solving the GLE (2.2a).

system associated with the operators in (3.1), for various values of `tol`. For this problem, we have $\|\mathcal{L}^{-1}\Pi\| = 0.8098$, indicating that no rescaling is necessary. The associated constant from (3.11) is given by $\gamma = 4.2576$. Figure 1a illustrates the effectiveness of the error bound presented in Theorem 3.6 for computing the Gramians via Algorithm 1. Notably, the ratio between the prescribed tolerance `tol` and the observed error for both Gramians remains below 10, highlighting the sharpness of the error estimate used to define the stopping criteria in Algorithm 1. In Figure 1b, we report the computational time (in seconds) required to execute Algorithm 1 as a function of the problem dimension n . Thanks to the use of sparse matrices, the runtime exhibits asymptotic linear growth, i.e., $\mathcal{O}(n)$. Overall, Figure 1 demonstrates that our implementation of Algorithm 1 efficiently delivers accurate approximations for any user-specified tolerance `tol`.

We observe that the exact Gramians of this example satisfy the set of LMIs (2.6) up to machine precision, indicating that the problem is well suited to ensure a quadratically stable ROM. Moreover, both \mathbf{A}_1 and \mathbf{A}_2 are normal matrices, so the hypothesis of Theorem 3.7 holds. The spectral condition numbers are $\kappa(\mathbf{A}_1) = 3$ and $\kappa(\mathbf{A}_2) = 2.4136$. Let us define the operators $\mathcal{M}_i : \mathbb{R}^{n \times n} \rightarrow \mathbb{R}^{n \times n}$

$$\mathcal{M}_i(\mathbf{X}) := \mathbf{A}_i \mathbf{X} + \mathbf{X} \mathbf{A}_i^\top + \mathbf{B}_i \mathbf{B}_i^\top, \quad i = 1, 2. \quad (5.2)$$

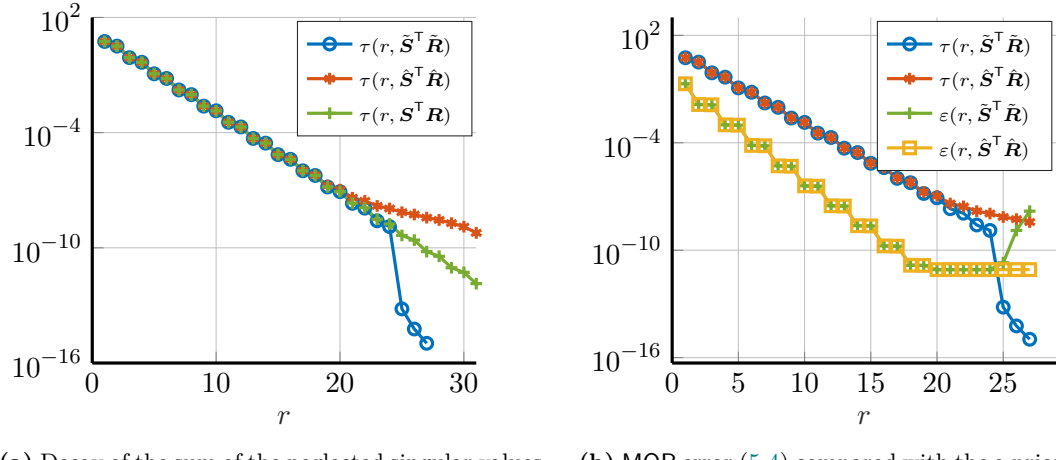
In Table 1, we report, for several values of the prescribed accuracy `tol`, the computed $\hat{\mu}$ (as defined in (3.28)) and the largest eigenvalue of the matrix in (5.2), with $i = 1, 2$. These quantities are shown for both the approximated reachability Gramian $\tilde{\mathcal{P}}$ and its perturbed counterpart $\hat{\mathcal{P}}$, which is adjusted to satisfy the LMIs, as described in Section 3.3.1. While $\tilde{\mathcal{P}}$ consistently fails to satisfy the LMIs, the perturbed version $\hat{\mathcal{P}}$ always fulfills them, thereby numerically validating Theorem 3.7.

Let us denote the cumulative sum of the neglected singular values as

$$\tau(r, \Upsilon) := 2 \sum_{k=r+1}^n \sigma_k(\Upsilon), \quad (5.3)$$

and

$$\eta(t) := \left(\int_0^t \|\mathbf{u}(s)\|_2^2 ds \right)^{\frac{1}{2}}, \quad \varepsilon(r, \Upsilon) := \left(\int_0^t \|\mathbf{y}(s) - \tilde{\mathbf{y}}(s)\|_2^2 ds \right)^{\frac{1}{2}} \eta(t)^{-1}, \quad (5.4)$$



(a) Decay of the sum of the neglected singular values, see (5.3). (b) MOR error (5.4) compared with the a priori error estimate of Theorem 2.4. Input $u = \sin(t^2 + t)$.

Figure 2 – Synthetic example (5.1) for $n = 200$. MOR for SLS through GLEs solution.

for $\Upsilon \in \{\tilde{S}^T \tilde{R}, \hat{S}^T \hat{R}\}$ where the output \tilde{y} is the one of the reduced system (1.4) of size r . For $n = 200$, we approximate the Gramians with $\text{tol} = 10^{-10}$ and display the results in Figure 2. The left plot shows the decay of the sum of the neglected singular values derived from the factors of the Gramian matrices. The green line corresponds to the exact Gramians, while the blue line represents the Gramians obtained by approximating the solution of the GLE. As expected, the green curve lies above the blue one since $\mathcal{P} \succeq \tilde{\mathcal{P}}$ and $\mathcal{Q} \succeq \tilde{\mathcal{Q}}$. This property follows directly from an application of [19, Thm. 3.3.16]. The right plot compares the actual output error (see (5.4)) with the error bound established in Theorem 2.4. When using the approximated Gramians $\tilde{\mathcal{P}}$ and $\tilde{\mathcal{Q}}$, the LMI condition is not satisfied. As a result, the error bound becomes unreliable, especially as we approach the smallest neglected singular values. In contrast, by using the perturbed Gramians $\hat{\mathcal{P}}$ and $\hat{\mathcal{Q}}$, which are explicitly constructed to satisfy the LMI, we obtain a ROM for which the error estimate (2.8) is rigorously verified.

5.2. Parametric Black-Scholes problem. The well-known (deterministic) Black-Scholes equation (see, e.g., [6]) has the following form:

$$\frac{\partial \psi}{\partial t} = \frac{1}{2} \nu^2 s^2 \frac{\partial^2 \psi}{\partial s^2} + \alpha s \frac{\partial \psi}{\partial s} - \alpha \psi, \quad s > L, \quad 0 < t \leq T, \quad (5.5)$$

for L, T given, where the unknown function $\psi(s, t)$ represents the fair price of the option when the corresponding asset price at time $T - t$ is s , and T is the maturity time of the option. Moreover, $\alpha \geq 0$ and $\nu > 0$ are given constants (representing the interest rate and the volatility, respectively). In practice, one considers a bounded spatial domain, setting $L < s < S$ for a sufficiently large S . We study (5.5) under the following conditions, which are a derivation from the European option call (see [21]) with initial data set to zero, i.e.,

$$\psi(L, t) = 0, \quad \psi(S, t) = S - e^{-\alpha t} K, \quad 0 \leq t \leq T. \quad (5.6)$$

Following the same strategy adopted in [20], we discretize the space on a uniform grid of $n = 1000$ points in the interval $[0, 200]$ with $K = 80$, using the classical centered finite

	$j = 1$	$j = 2$	$j = 3$	$j = 4$
$\lambda_1(\mathcal{N}_j(\tilde{Q}_j))$	$1.1 \cdot 10^{-5}$	$2.9 \cdot 10^{-7}$	$1.5 \cdot 10^{-5}$	$3.6 \cdot 10^{-7}$
$\lambda_1(\mathcal{N}_j(\hat{Q}_j))$	$1.6 \cdot 10^{-11}$	$6.8 \cdot 10^{-13}$	$2.3 \cdot 10^{-11}$	$5.6 \cdot 10^{-13}$

Table 2 – Parametric Black-Scholes problem (5.7). The table shows the largest eigenvalue of (5.8) for each system mode.

difference scheme. We thus have the following discrete matrices

$$\mathbf{A}(\nu, \alpha) = \frac{\nu^2}{2} \mathbf{D} + \alpha \mathbf{G}, \quad \mathbf{B}(\nu, \alpha) = \begin{bmatrix} S\nu^2 \mathbf{B}_1^\top + \alpha \mathbf{B}_2^\top \\ -K\nu^2 \mathbf{B}_1^\top + \alpha \mathbf{B}_2^\top \end{bmatrix}^\top, \quad \mathbf{C} = \begin{bmatrix} \frac{1}{n}, \dots, \frac{1}{n} \\ 0, \dots, 1 \end{bmatrix}, \quad (5.7)$$

where the output matrix \mathbf{C} accounts for the average fair price of the option and its value at the boundary $s = S$, \mathbf{B}_1 and \mathbf{B}_2 arise from the boundary conditions (5.6). Furthermore, the matrices \mathbf{D} and \mathbf{G} correspond to the discretization of the diffusion and convection–reaction terms, respectively. To generate a switches system, we consider $M = 4$ parameter samples $\boldsymbol{\mu}_i := (\nu_i, \alpha_i)$ given by

$$\boldsymbol{\mu}_1 = [0.25, 0.001], \quad \boldsymbol{\mu}_2 = [0.05, 0.02], \quad \boldsymbol{\mu}_3 = [0.25, 0.02], \quad \boldsymbol{\mu}_4 = [0.05, 0.001].$$

We apply the PBR method described in Section 4 to the resulting SLS, setting $\text{tol} = 10^{-8}$ and normalizing the input matrices $\mathbf{B}(\nu, \alpha)$.

First, we want to verify the effectiveness of the procedure described in Section 4.4 to tighten the LMIs. With this aim, let us define the matrix operator $\mathcal{N}_i : \mathbb{R}^{n \times n} \rightarrow \mathbb{R}^{n \times n}$

$$\mathcal{N}_j(\mathbf{X}) := \mathbf{A}_j^\top \mathbf{X} + \mathbf{X} \mathbf{A}_j + \mathbf{C}^\top \mathbf{C}^\top, \quad j = 1, \dots, 4. \quad (5.8)$$

Table 2 displays the largest eigenvalue of \mathcal{N}_j for each system mode. Using the modified Gramians (4.13) successfully reduces the magnitude of the largest eigenvalues by several orders. Next, we compare the FOM with the ROM considering the input functions

$$\mathbf{u}_1(t) := \begin{bmatrix} 1 & e^{-0.02t} \end{bmatrix}^\top \quad \text{and} \quad \mathbf{u}_2(t) := \begin{bmatrix} \sin(2\pi e^{\frac{t}{2}}) & \sin(2\pi e^{\frac{t}{2}}) \end{bmatrix}^\top. \quad (5.9)$$

Results for the two input functions are displayed in Figure 3 for a switching signal with 10 randomly chosen switching times. For both input functions, the ROM output with $r = 30$ qualitatively overlaps with the FOM. With the aim of showing the different error bound terms in Theorem 4.3, we introduce the following functions:

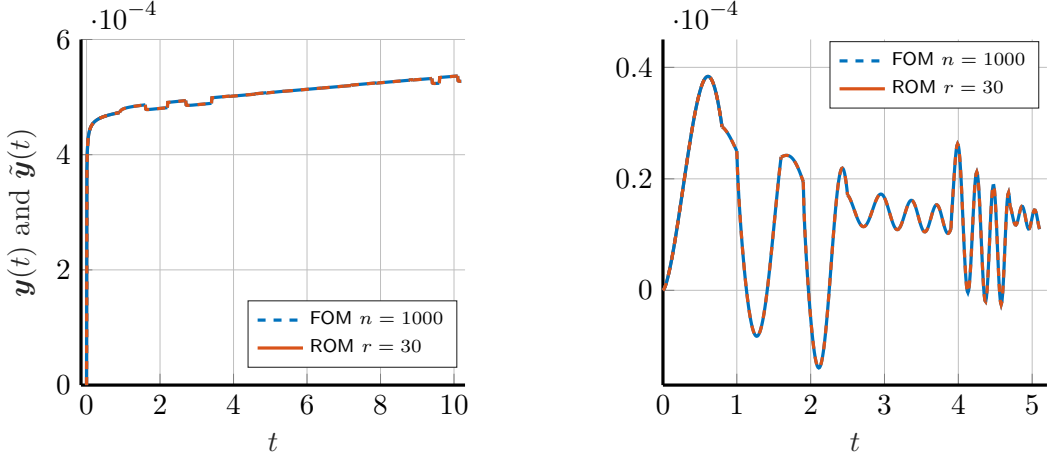
$$\tau(r, \Upsilon) := 2 \sum_{k=r+1}^{\tilde{n}} \tilde{\sigma}_k, \quad (5.10)$$

$$\chi(r, \Upsilon) := \eta(t)^{-1} \sum_{k=r+1}^{\tilde{n}} \mathcal{H}_{c,o,q}(s_{k+1}, s_k)^{\frac{1}{2}} H(\mathcal{H}_{c,o,q}(s_{k+1}, s_k)), \quad (5.11)$$

$$\iota(r, \Upsilon) := -\eta(t)^{-1} \sum_{k=r+1}^{\tilde{n}} \mathcal{G}_{c,o,q}(s_{k+1}, s_k)^{\frac{1}{2}} H(-\mathcal{G}_{c,o,q}(s_{k+1}, s_k)), \quad (5.12)$$

$$\varphi(r, \Upsilon) := \tau(r; \Upsilon) + \chi(r; \Upsilon) + \iota(r; \Upsilon), \quad (5.13)$$

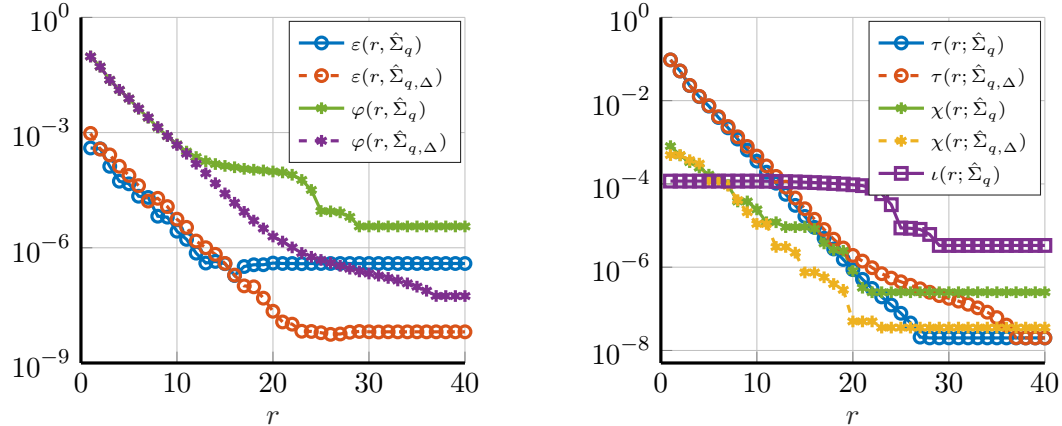
for $\Upsilon \in \{\hat{\Sigma}_q, \hat{\Sigma}_{q,\Delta}\}$, i.e., either we use the PBR-ROM (4.2) (denoted by $\hat{\Sigma}_q$) or the PBR-ROM with suitable perturbed Gramians derived in Section 4.4 (denoted by $\hat{\Sigma}_{q,\Delta}$).



(a) Qualitative comparison of the first component of the full and reduced output with input signal \mathbf{u}_1 as in (5.9) and 20 switching points.

(b) Qualitative comparison of the second component of the full and reduced outputs with input signal \mathbf{u}_2 as in (5.9) and 10 switching points.

Figure 3 – Example derived from the Black-Scholes model for $n = 1000$. The GLEs are solved with tolerance $\text{tol} = 10^{-8}$.



(a) Decay of the error (5.4) and of the error estimate (5.13) for the PBR obtained from $\tilde{\mathcal{P}}(t)$, $\tilde{\mathcal{Q}}(t)$ (see (4.4)) and $\hat{\mathcal{P}}(t)$, $\hat{\mathcal{Q}}(t)$ (see Section 4.4).

(b) The components (5.10), (5.11), (5.12) of the error estimate (5.13) for the ROM $\hat{\Sigma}_q$ and the ROM $\hat{\Sigma}_{q,\Delta}$.

Figure 4 – Example derived from the Black-Scholes model for $n = 1000$. GLE solved with $\text{tol} = 10^{-8}$, input function \mathbf{u}_2 defined in (5.9), and $K = 10$ switches times.

Figure 4a shows the actual errors and their corresponding estimators for the two ROMs. As expected, the error bounds lie above the actual errors in all cases. Notably, the ROM $\hat{\Sigma}_{q,\Delta}$ obtained using perturbed Gramians exhibits greater accuracy than $\hat{\Sigma}_q$, both in terms of the actual error and its estimate, when the reduced dimension r is sufficiently large. This behaviour is explained in **Figure 4b**, where the error bound is broken down into its three components. For the PBR ROM $\hat{\Sigma}_q$, the dominant contribution to the error bound at higher values of r stems from the violation of the LMI conditions, i.e., the

component $\iota(r, \hat{\Sigma}_q)$. In contrast, we found that this contribution is negligible (around machine precision) for $\hat{\Sigma}_{q,\Delta}$, and thus we do not display it.

6. CONCLUSIONS AND PERSPECTIVES

Given a prescribed user tolerance tol , we present a procedure to efficiently compute an approximation $\tilde{\mathbf{X}}$ to the solution \mathbf{X} of the GLE (1.1), ensuring that $\|\mathbf{X} - \tilde{\mathbf{X}}\|_2 \leq \text{tol}$ by deriving suitable error bound; cf. [Theorem 3.6](#). This strategy is subsequently employed in the context of MOR for SLS, where the ROM is obtained by balancing the complete SLS using the solutions of two GLE. Under suitable LMI conditions satisfied by the exact solutions of the GLE, this procedure guarantees stability as well as an a priori error bound. For a particular class of SLS, we demonstrate in [Theorem 3.7](#) that the derived error estimate is essential for constructing stable and error-certified ROM when starting from approximate solutions of the GLE.

The assumption that the precise solutions of GLE meet the LMI is indeed restrictive. To address this limitation, we derive an innovative error bound in [Theorem 4.3](#) that accounts for scenarios in which the LMI may not hold. To manage the error growth from inexact LMI, we introduce in [Section 4.1](#) a novel ROM, termed piecewise balance reduction (PBR) for SLS, based on a time-dependent piecewise-constant projection basis. The projection basis is derived from the solution of multiple GLEs and the following application of a balancing-type reduction method. The novel error bound also accounts for the use of piecewise-constant projection matrices, which constitute a novel source of error. Finally, we confirmed the efficacy of our methodology and theoretical findings through numerical experiments.

In future work, we want to apply the novel PBR methodology in two different contexts. First, to derive stable and accurate surrogate models for switched differential-algebraic equations, and second, to accelerate model predictive control for SLS.

ACKNOWLEDGMENT

MM acknowledges funding by the BMBF (grant no. 05M22VSA) and acknowledges support by the Stuttgart Center for Simulation Science. BU is funded by Deutsche Forschungsgemeinschaft (DFG, German Research Foundation) – Project-ID 258734477 – SFB 1173. Major parts of this manuscript were written while both authors were affiliated with the Stuttgart Center for Simulation Science at the University of Stuttgart.

REFERENCES

- [1] A. C. ANTOULAS. *Approximation of large-scale dynamical systems*. Adv. Des. Control. Society for Industrial and Applied Mathematics, Philadelphia, PA, USA, 2005.
- [2] M. BAŞTUĞ, M. PETRECKÝ, R. WISNIEWSKI, AND J. LETH. *Model reduction by nice selections for linear switched systems*. *IEEE Trans. Automat. Control*, 61(11):3422–3437, 2016.
- [3] P. BENNER AND T. BREITEN. *Interpolation-based \mathcal{H}_2 -model reduction of bilinear control systems*. *SIAM J. Matrix Anal. Appl.*, 33(3):859–885, 2012.
- [4] P. BENNER AND T. BREITEN. *Low rank methods for a class of generalized Lyapunov equations and related issues*. *Numer. Math.*, 124:441–470, 2013.
- [5] P. BENNER AND T. DAMM. *Lyapunov equations, energy functionals, and model order reduction of bilinear and stochastic systems*. *SIAM J. Cont. Optim.*, 49(2):686–711, 2011.
- [6] F. BLACK AND M. SCHOLES. *The pricing of options and corporate liabilities*. *Journal of Political Economy*, 81(3):637–654, 1973.

- [7] T. BREITEN AND E. RINGH. Residual-based iterations for the generalized Lyapunov equation. *BIT Numer. Math.*, 59:823–852, 2019.
- [8] D. CHENG. Stabilization of planar switched systems. *Systems Control Lett.*, 51:79–88, 2004.
- [9] M. CONDON AND R. IVANOV. Nonlinear systems – algebraic Gramians and model reduction. *Compel*, 24(1):202–219, 2005.
- [10] T. DAMM. Direct methods and ADI-preconditioned Krylov subspace methods for generalized Lyapunov equations. *Numer. Lin. Alg. Appl.*, 15(9):853–871, 2008.
- [11] T. DAMM AND D. HINRICHSEN. Newton’s method for a rational matrix equation occurring in stochastic control. *Linear Algebra and its Applications*, 332–334:81–109, 2001.
- [12] T. DAMM. *Rational Matrix Equations in Stochastic Control*. Lecture Notes in Control and Information Sciences. Springer-Verlag, 2004.
- [13] G. DULLERUD AND F. PAGANINI. *A Course in Robust Control Theory a convex approach*. 01 2000.
- [14] N. GILLIS AND P. SHARMA. On computing the distance to stability for matrices using linear dissipative Hamiltonian systems. *Automatica J. IFAC*, 85:113–121, 2017.
- [15] I. V. GOSEA, M. PETRECKY, AND A. C. ANTOULAS. Data-driven model order reduction of linear switched systems in the Loewner framework. *SIAM J. Sci. Comput.*, 40(2):B572–B610, 2018.
- [16] I. V. GOSEA, M. PETRECKY, A. C. ANTOULAS, AND C. FITER. Balanced truncation for linear switched systems. *Adv. Comput. Math.*, 44(6):1845–1886, 2018.
- [17] I. V. GOSEA, I. PONTES DUFF, P. BENNER, AND A. C. ANTOULAS. Model order reduction of switched linear systems with constrained switching. In J. FEHR AND B. HAASDONK, editors, *IUTAM Symposium on Model Order Reduction of Coupled Systems, Stuttgart, Germany, May 22–25, 2018*, volume 36 of *IUTAM Bookseries*, pages 41–53. Springer-Verlag, 2020.
- [18] W. S. GRAY AND J. MESKO. Energy functions and algebraic Gramians for bilinear systems. *IFAC Proceedings Volumes*, 31(17):101–106, 1998.
- [19] R. A. HORN AND C. R. JOHNSON. *Topics in Matrix Analysis*. Cambridge University Press, 1991.
- [20] K. J. IN ’T HOUT AND J. A. C. WEIDEMAN. A contour integral method for the black–scholes and heston equations. *SIAM Journal on Scientific Computing*, 33(2):763–785, 2011.
- [21] K. J. IN ’T HOUT AND B. D. WELFERT. Stability of adi schemes applied to convection-diffusion equations with mixed derivative terms. *Applied Numerical Mathematics*, 57(1):19–35, 2007.
- [22] I. M. JAIMOUKHA AND E. M. KASENALLY. Krylov subspace methods for solving large lyapunov equations. *SIAM Journal on Numerical Analysis*, 31(1):227–251, 1994.
- [23] E. JARLEBRING, G. MELE, D. PALITTA, AND E. RINGH. Krylov methods for low-rank commuting generalized Sylvester equations. *Numer. Lin. Alg. Appl.*, 28(6):e2176, 2018.
- [24] M. KARTMANN, M. MANUCCI, B. UNGER, AND S. VOLKWEIN. Certified model predictive control for switched evolution equations using model order reduction, 2024. arXiv 2412.12930.
- [25] D. KRESSNER AND P. SIRKOVIĆ. Truncated low-rank methods for solving general linear matrix equations. *Numer. Lin. Alg. Appl.*, 22(3):564–583, 2015.
- [26] P. LANCASTER AND M. TISMANETSKY. *The Theory of Matrices: With Applications*. Computer Science and Scientific Computing. Elsevier Science, 2 edition, 1985.
- [27] R. B. LEHOUQCQ, D. C. SORENSEN, AND C. YANG. *ARPACK Users’ Guide*. Society for Industrial and Applied Mathematics, 1998.
- [28] D. LIBERZON. *Switching in Systems and Control*. Springer Science & Business Media, New York, NY, USA, 2003.
- [29] N. MONSHIZADEH, H. L. TRENTELMAN, AND M. K. CAMLIBEL. A simultaneous balanced truncation approach to model reduction of switched linear systems. *IEEE Trans. Automat. Control*, 47(12):3118–3131, 2012.
- [30] A. V. PAPADOPOULOS AND M. PRANDINI. Model reduction of switched affine systems: a method based on balanced truncation and randomized optimization. In *Proc. 17th Int. Conf. Hybrid Syst. Comput. Control*, pages 113–122, Berlin, Germany, 2014.
- [31] A. V. PAPADOPOULOS AND M. PRANDINI. Model reduction of switched affine systems. *Automatica J. IFAC*, 70:57–65, 2016.
- [32] S. PEITZ AND S. KLUS. Koopman operator-based model reduction for switched-system control of PDEs. *Automatica J. IFAC*, 106:184–101, 2019.

- [33] M. PETRECZKY AND I. V. GOSEA. *Model reduction and realization theory of linear switched systems*. In C. BEATTIE, P. BENNER, M. EMBREE, S. GUGERCIN, AND S. LEFTERIU, editors, *Realization and Model Reduction of Dynamical Systems*, pages 197–212. Springer-Verlag, 2022.
- [34] M. PETRECZKY, R. WISNIEWSKI, AND J. LETH. *Balanced truncation for linear switched systems*. *Nonlinear Anal. Hybrid Syst.*, 10:4–20, 2013.
- [35] I. PONTES DUFF, S. GRUNDEL, AND P. BENNER. *New Gramians for switched linear systems: Reachability, observability, and model reduction*. *IEEE Trans. Automat. Control*, 65(6):2526–2535, 2020.
- [36] Y. SAAD. *Numerical solution of large Lyapunov equations*. In *Proceedings of the international symposium MTNS-89 signal processing, scattering, operator theory, and numerical methods.*, 1990.
- [37] H. SANDBERG. Model reduction for linear time-varying systems. *Ph.D. Thesis, Lund Institute of Technology, Sweden*, 2004.
- [38] G. SCARCIOTTI AND A. ASTOLFI. *Model reduction for hybrid systems with state-dependent jumps*. *IFAC-PapersOnLine*, 49(18):850–855, 2016.
- [39] H. SCHNEIDER. *Positive operators and an inertia theorem*. *Numer. Math.*, 7:11–17, 1965.
- [40] P. SCHULZE AND B. UNGER. *Model reduction for linear systems with low-rank switching*. *SIAM J. Cont. Optim.*, 56(6):4365–4384, 2018.
- [41] H. SCHWETLICK AND U. SCHNABEL. *Iterative computation of the smallest singular value and the corresponding singular vectors of a matrix*. *Linear Algebra Appl.*, 371:1–30, 2003.
- [42] H. R. SHAKER AND R. WISNIEWSKI. *Model reduction of switched systems based on switching generalized Gramians*. *Int. J. Innov. Comput. I.*, 8(7(B)):5025–5044, 2012.
- [43] S. D. SHANK, V. SIMONCINI, AND D. B. SZYLD. *Efficient low-rank solution of generalized Lyapunov equations*. *Numer. Math.*, 134(2):327–342, 2016.
- [44] V. SIMONCINI. *A new iterative method for solving large-scale lyapunov matrix equations*. *SIAM Journal on Scientific Computing*, 29(3):1268–1288, 2007.
- [45] V. SIMONCINI. *Computational methods for linear matrix equations*. *SIAM Rev.*, 58(3):377–441, 2016.
- [46] W. M. WONHAM. *On a matrix Riccati equation of stochastic control*. *SIAM J. Cont.*, 6(4):681–697, 1968.
- [47] L. WU AND W. X. ZHENG. *Weighted \mathcal{H}_∞ model reduction for linear switched systems with time-varying delay*. *Automatica J. IFAC*, 45:186–193, 2009.

APPENDIX A. TECHNICAL PROOFS

A.1. Proof of Lemma 4.2. Consider a switching signal $q(t) \in \mathcal{S}$ and the associated discrete set of times $t_k \in \tilde{\mathcal{T}}_{q(t)} := \mathcal{T}_{q(t)} \cup \{t_0, t_{K+1}\}$, where $\mathcal{T}_{q(t)}$ is the set of switching times t_k for $k = 1, \dots, K$, and $t_0 := 0$, $t_{K+1} := t$. Let us define

$$z(t) := \mathbf{A}_{q(t_k^+), 21} \tilde{\mathbf{x}}(t) + \mathbf{B}_{q(t_k^+), 2} \mathbf{u}(t), \quad t \in [t_k, t_{k+1}), \quad k = 0, \dots, K$$

where we used the notation introduced in (4.6), and observe that

$$\dot{\mathbf{x}}_o(t) = \bar{\mathbf{A}}_{q(t_k^+)} \mathbf{x}_o(t) + \begin{bmatrix} \mathbf{0} \\ z(t) \end{bmatrix}, \quad \dot{\mathbf{x}}_c(t) = \bar{\mathbf{A}}_{q(t_k^+)} \mathbf{x}_c(t) - \begin{bmatrix} \mathbf{0} \\ z(t) \end{bmatrix} + 2\bar{\mathbf{B}}_{q(t_k^+)} \mathbf{u}(t) \quad (\text{A.1})$$

with $\dot{\mathbf{x}}_o$ and $\dot{\mathbf{x}}_c(t)$ as defined in (4.7). Note that $\bar{\mathbf{C}}_{q(t)} \mathbf{x}_o(t) = \bar{\mathbf{y}}(t) - \tilde{\mathbf{y}}(t)$ and for $t \in (t_k, t_{k+1})$ we have

$$\begin{aligned} \frac{d}{dt} \left(\mathbf{x}_o^\top(t) \Sigma_{q(t_k^+)} \mathbf{x}_o(t) \right) &= 2\mathbf{x}_o^\top(t) \bar{\mathbf{A}}_{q(t_k^+)}^\top \Sigma_{q(t_k^+)} \mathbf{x}_o(t) + 2\sigma(q(t_k^+)) z(t)^\top \bar{\mathbf{x}}_2(t) \\ &\leq \lambda_1(\mathbf{M}_o(q(t_k^+))) \|\mathbf{x}(t)\|_2^2 - \mathbf{x}_o^\top(t) \bar{\mathbf{C}}_{q(t_k^+)}^\top \bar{\mathbf{C}}_{q(t_k^+)} \mathbf{x}_o(t) + 2\sigma(q(t_k^+)) z(t)^\top \bar{\mathbf{x}}_2(t), \end{aligned} \quad (\text{A.2})$$

where we exploited definition (4.8), i.e. it holds

$$\mathbf{x}(t)^\top \left(\bar{\mathbf{A}}_j^\top \Sigma_j + \Sigma_j \bar{\mathbf{A}}_j + \bar{\mathbf{C}}_j^\top \bar{\mathbf{C}}_j \right) \mathbf{x}(t) \preceq \lambda_1(\mathbf{M}_o(j)) \|\mathbf{x}_o(t)\|_2^2,$$

for all $j \in \mathcal{J}$. Integrating (A.2) over the interval (t_k, t_{k+1}) we get

$$\begin{aligned} \tilde{\mathcal{G}}_o(q(t_k^+)) &:= \mathbf{x}_o^\top(t_{k+1}^-) \boldsymbol{\Sigma}_{q(t_k^+)} \mathbf{x}_o(t_{k+1}^-) - \mathbf{x}_o^\top(t_k^+) \boldsymbol{\Sigma}_{q(t_k^+)} \mathbf{x}_o(t_k^+) \\ &= \int_{t_k}^{t_{k+1}} \frac{d}{dt} \left(\mathbf{x}_o^\top(s) \boldsymbol{\Sigma}_{q(t_k^+)} \mathbf{x}_o(s) \right) ds \leq \int_{t_k}^{t_{k+1}} \lambda_1(\mathbf{M}_o(q(t_k^+))) \|\mathbf{x}(s)\|_2^2 ds \\ &\quad - \int_{t_k}^{t_{k+1}} \mathbf{x}_o^\top(s) \bar{\mathbf{C}}_{q(t_k^+)}^\top \bar{\mathbf{C}}_{q(t_k^+)} \mathbf{x}_o(s) ds + \int_{t_k}^{t_{k+1}} 2\sigma(q(t_k^+)) \mathbf{z}(s)^\top \bar{\mathbf{x}}_2(s) ds, \end{aligned} \quad (\text{A.3})$$

and reordering the terms we find

$$\begin{aligned} \int_{t_k}^{t_{k+1}} \|\bar{\mathbf{y}}(s) - \tilde{\mathbf{y}}(s)\|_2^2 ds &\leq -\tilde{\mathcal{G}}_o(q(t_k^+)) + \lambda_1(\mathbf{M}_o(q(t_k^+))) \int_{t_k}^{t_{k+1}} \|\mathbf{x}_o(s)\|_2^2 ds \\ &\quad + 2\sigma(q(t_k^+)) \int_{t_k}^{t_{k+1}} \mathbf{z}(s)^\top \bar{\mathbf{x}}_2(s) ds. \end{aligned} \quad (\text{A.4})$$

Next, we use definition (4.7) for $\mathbf{M}_c(j)$, we multiply from left and right by $\boldsymbol{\Sigma}_j^{-1}$ and we find for all $j \in \mathcal{J}$ that

$$\boldsymbol{\Sigma}_j^{-1} \bar{\mathbf{A}}_j + \bar{\mathbf{A}}_j^\top \boldsymbol{\Sigma}_j^{-1} + \boldsymbol{\Sigma}_j^{-1} \bar{\mathbf{B}}_j \bar{\mathbf{B}}_j^\top \boldsymbol{\Sigma}_j^{-1} - \lambda_1(\mathbf{M}_c(j)) \boldsymbol{\Sigma}_j^{-2} \preceq \mathbf{0}. \quad (\text{A.5})$$

Using the Schur complement it follows that (A.5) is equivalent to

$$\begin{bmatrix} \boldsymbol{\Sigma}_j^{-1} \bar{\mathbf{A}}_j + \bar{\mathbf{A}}_j^\top \boldsymbol{\Sigma}_j^{-1} - \lambda_1(\mathbf{M}_c(j)) \boldsymbol{\Sigma}_j^{-2} & \boldsymbol{\Sigma}_j^{-1} \bar{\mathbf{B}}_j \\ \bar{\mathbf{B}}_j^\top \boldsymbol{\Sigma}_j^{-1} & -\mathbf{I} \end{bmatrix} \preceq \mathbf{0},$$

then, by definition (A.1), it follows for $t \in (t_k, t_{k+1})$ that

$$\begin{aligned} &\frac{d}{dt} \left(\mathbf{x}_c^\top(t) \boldsymbol{\Sigma}_{q(t_k^+)}^{-1} \mathbf{x}_c(t) \right) \\ &= \begin{bmatrix} \mathbf{x}_c(t) \\ 2\mathbf{u}(t) \end{bmatrix}^\top \begin{bmatrix} \boldsymbol{\Sigma}_{q(t_k^+)}^{-1} \bar{\mathbf{A}}_{q(t_k^+)} + \bar{\mathbf{A}}_{q(t_k^+)}^\top \boldsymbol{\Sigma}_{q(t_k^+)}^{-1} - \lambda_1(\mathbf{M}_c(q(t_k^+))) \boldsymbol{\Sigma}_{q(t_k^+)}^{-2} & \boldsymbol{\Sigma}_{q(t_k^+)}^{-1} \bar{\mathbf{B}}_{q(t_k^+)} \\ \bar{\mathbf{B}}_{q(t_k^+)}^\top \boldsymbol{\Sigma}_{q(t_k^+)}^{-1} & -\mathbf{I} \end{bmatrix} \begin{bmatrix} \mathbf{x}_c(t) \\ 2\mathbf{u}(t) \end{bmatrix} \\ &\quad + 4\|\mathbf{u}(t)\|_2^2 + \lambda_1(\mathbf{M}_c(q(t_k^+))) \mathbf{x}_c(t)^\top \boldsymbol{\Sigma}_{q(t_k^+)}^{-2} \mathbf{x}_c(t) - 2\mathbf{x}_c(t)^\top \boldsymbol{\Sigma}_{q(t_k^+)}^{-1} \begin{bmatrix} \mathbf{0} \\ \mathbf{z}(t) \end{bmatrix} \\ &\leq \lambda_1(\mathbf{M}_c(q(t_k^+))) \frac{1}{\sigma(q(t_k^+))^2} \|\mathbf{x}_c(t)\|_2^2 + 4\|\mathbf{u}(t)\|_2^2 - 2 \frac{1}{\sigma(q(t_k^+))} \mathbf{z}(t)^\top \bar{\mathbf{x}}_2(t) \end{aligned}$$

where we also used the fact that $\mathbf{x}_c(t) \boldsymbol{\Sigma}_{q(t_k^+)}^{-1} [\mathbf{0} \ \mathbf{z}(t)]^\top = \sigma(q(t_k^+))^{-1} \mathbf{z}(t)^\top \bar{\mathbf{x}}_2(t)$. Now we integrate over the interval (t_k, t_{k+1}) and we get

$$\begin{aligned} \tilde{\mathcal{G}}_c(q(t_k^+)) &:= \mathbf{x}_c^\top(t_{k+1}^-) \boldsymbol{\Sigma}_{q(t_k^+)}^{-1} \mathbf{x}_c(t_k^-) - \mathbf{x}_c^\top(t_k^+) \boldsymbol{\Sigma}_{q(t_k^+)}^{-1} \mathbf{x}_c(t_k^+) = \int_{t_k}^{t_{k+1}} \frac{d}{dt} \left(\mathbf{x}_c^\top(s) \boldsymbol{\Sigma}_{q(t_k^+)}^{-1} \mathbf{x}_c(s) \right) ds \\ &\leq 4 \int_{t_k}^{t_{k+1}} \|\mathbf{u}(s)\|_2^2 ds - 2 \int_{t_k}^{t_{k+1}} \frac{1}{\sigma(q(t_k^+))} \mathbf{z}(s)^\top \bar{\mathbf{x}}_2(s) ds \\ &\quad + \lambda_1(\mathbf{M}_c(q(t_k^+))) \frac{1}{\sigma(q(t_k^+))^2} \int_{t_k}^{t_{k+1}} \|\mathbf{x}_c(s)\|_2^2 ds, \end{aligned}$$

and after rearranging the terms we have the relation

$$\begin{aligned} 2 \int_{t_k}^{t_{k+1}} \mathbf{z}(s)^\top \bar{\mathbf{x}}_2(s) \, ds &\leq -\tilde{\sigma}(q(t_k^+)) \tilde{\mathcal{G}}_c(q(t_k^+)) + 4\sigma(q(t_k^+)) \int_{t_k}^{t_{k+1}} \|\mathbf{u}(s)\|_2^2 \, ds \\ &\quad + \lambda_1(\mathbf{M}_c(q(t_k^+))) \frac{1}{\sigma(q(t_k^+))} \int_{t_k}^{t_{k+1}} \|\mathbf{x}_c(s)\|_2^2 \, ds. \end{aligned} \quad (\text{A.6})$$

Multiplying (A.6) by $\sigma(q(t_k^+))$ and then substituting into (A.4) we get

$$\begin{aligned} \int_{t_k}^{t_{k+1}} \|\bar{\mathbf{y}}(s) - \tilde{\mathbf{y}}(s)\|_2^2 \, ds &\leq 4\sigma(q(t_k^+))^2 \int_{t_k}^{t_{k+1}} \|\mathbf{u}(s)\|_2^2 \, ds \\ &\quad - \tilde{\mathcal{G}}_o(q(t_k^+)) - \sigma(q(t_k^+))^2 \tilde{\mathcal{G}}_c(q(t_k^+)) \\ &\quad + \lambda_1(\mathbf{M}_o(q(t_k^+))) \int_{t_k}^{t_{k+1}} \|\mathbf{x}_o(s)\|_2^2 \, ds + \lambda_1(\mathbf{M}_c(q(t_k^+))) \int_{t_k}^{t_{k+1}} \|\mathbf{x}_c(s)\|_2^2 \, ds. \end{aligned} \quad (\text{A.7})$$

Finally, repeating the previous passages for all $k = 0, \dots, K$, summing up all the relations of type (A.7), and recalling the definition (4.8) for $\mathcal{G}_{o,q}(n, r)$, $\mathcal{G}_{c,q}(n, r)$, $\mathcal{H}_{o,q}(n, r)$, and $\mathcal{H}_{c,q}(n, r)$ we end with

$$\int_0^t \|\bar{\mathbf{y}}(s) - \tilde{\mathbf{y}}(s)\|_2^2 \, ds \leq \mathcal{H}_{o,q}(n, r) + \mathcal{H}_{c,q}(n, r) - \mathcal{G}_{o,q}(n, r) - \mathcal{G}_{c,q}(n, r) + 4\tilde{\sigma}^2 \int_0^t \|\mathbf{u}(s)\|_2^2 \, ds,$$

that corresponds to statement (4.9) by noticing that $\mathbf{y} \equiv \bar{\mathbf{y}}$.

* INSTITUTE FOR APPLIED AND NUMERICAL MATHEMATICS, KARLSRUHE INSTITUTE OF TECHNOLOGY, 76131 KARLSRUHE, GERMANY

Email address: {mattia.manucci,benjamin.unger}@kit.edu